Summer 2021

Advanced control techniques for modern inertia based inverters

Sepehr Saadatman

Department: Electrical and Computer Engineering

ADVANCED CONTROL TECHNIQUES FOR MODERN INERTIA BASED INVERTERS

by

SEPEHR SAADATMAND

A DISSERTATION

Presented to the Graduate Faculty of the

MISSOURI UNIVERSITY OF SCIENCE AND TECHNOLOGY

In Partial Fulfillment of the Requirements for the Degree

DOCTOR OF PHILOSOPHY

in

ELECTRICAL ENGINEERING

2021

Approved by:

Pourya Shamsi, Advisor
Mehdi Ferdowsi
Jonathan Kimball
Rui Bo
Ali Rownaghi

PUBLICATION DISSERTATION OPTION

This dissertation consists of the following three articles, formatted in the style used by the Missouri University of Science and Technology:

Paper I, found on pages 5–32, has been published in IEEE Transaction of Industrial Electronics, in May 2020.

Paper II, found on pages 33–66, has been published in the International Journal of Electrical Power and Energy System, Elsevier, Dec 2020.

Paper III, found on pages 67–96, is submitted to IEEE Journal of Selected and Emerging Topics in Industrial Electronics.

ABSTRACT

In this research three artificial intelligent (AI)-based techniques are proposed to regulate the voltage and frequency of a grid-connected inverter. The increase in the penetration of renewable energy sources (RESs) into the power grid has led to the increase in the penetration of fast-responding inertia-less power converters. The increase in the penetration of these power electronics converters changes the nature of the conventional grid, in which the existing kinetic inertia in the rotating parts of the enormous generators plays a vital role. The concept of virtual inertia control scheme is proposed to make the behavior of grid connected inverters more similar to the synchronous generators, by mimicking the mechanical behavior of a synchronous generator. Conventional control techniques lack to perform optimally in nonlinear, uncertain, inaccurate power grids. Besides, the decoupled control assumption in conventional VSGs makes them nonoptimal in resistive grids.

The neural network predictive controller, the heuristic dynamic programming, and the dual heuristic dynamic programming techniques are presented in this research to overcome the draw backs of conventional VSGs. The nonlinear characteristics of neural networks, and the online training enable the proposed methods to perform as robust and optimal controllers. The simulation and the experimental laboratory prototype results are provided to demonstrate the effectiveness of the proposed techniques.

ACKNOWLEDGMENTS

First, I would like to thank my family, my parents, brother, and my lovely wife, who have always been supportive, caring, and helpful. They have always been encouraging me to do better, and to be successful.

I would like to express my special gratitude to my PhD advisor Dr. Pourya Shamsi and my co-advisor Dr. Mehdi Ferdowsi. I would not be here if they had not believed in me and trusted me. They have been supporting me in all aspects of my life, including technical support, financial support, and so other perspectives of my life for the past three years.

I would like to thank my committee members, Dr. Jonathan Kimball and Dr. Rui Bo. During my PhD studies, I was lucky to get the chance to cooperate in the extreme fast charging project. I have learnt a lot, gained a great variety of experiences, and used their valuable advises. Moreover, I would like to thank Dr. Ali Rownaghi for accepting to be a member of my technical committee and giving me several appreciated recommends. My journey in the machine learning world would not be started if it were not for Dr. Donald Wunsch's suggestions, and I will always be grateful for his support and recommendations.

Finally, I would like to thank all the friends who have helped to finish my long academic journey.

TABLE OF CONTENTS

LIST OF ILLUSTRATIONS

PAPER I Page

PAPER II

LIST OF TABLES

NOMENCLATURE

Symbol	Description
RES	Renewable Energy Source
SG	Synchronous Generator
VSG	Virtual Synchronous Generator
PLL	Phase-Locked Loop
PI	Proportional Integral
NNPC	Neural Network Predictive Controller
MPC	Model Predictive Controller
HDP	Heuristic Dynamic Programming
ACD	Adaptive Critic Design
DHP	Dual Heuristic Programming
PV	Photovoltaic
VSG	Voltage Source Converter
W	Kinetic Energy
J	Moment of Inertia
ω_m	Rotational Speed
P_{in}	Input Power
P_{out}	Output Power
θ_m	Rotational Angle
Q_{ref}	Reactive Power Reference
Q_{out}	Reactive Power Output

D_q	Voltage Droop Coefficient
k	Regulation Factor
E	Inverter Voltage Amplitude
L_f	Filter Inductance
R_f	Filter Resistance
L_l	Line Inductance
R_l	Line Resistance
Z_{eq}	Equivalent Impedance
δ	Power Angle
$Xc(t)$	State Space Vector
$Uc(t)$	Control VEctor
$Yc(t)$	Output Vector
T_s	Sampling Time
γ	Discount Factor
W_i	Neural Network Weight Matrix
b_i	Neural Network Bias Vector

SECTION

1. INTRODUCTION

The concern regarding the environmental and energy crisis has been increase during the last decades. Therefore, the penetration of renewable energy sources (RESs) into the power grid, as clean a source of energy, have been increased significantly. The most conventional approach to integrate renewable energy resources into the power grid is through grid-connected inverters. The conventional method to control a grid-connected inverter is through the utilization of the direct current/power regulation control scheme. The fast-responding and inertia-less inherence of the conventional power electronics converter distinguish them from conventional synchronous generators (SGs), as the main source of generation in the power grid. The increase in penetration of power electronics-based renewable energy resources into the power grid changes the power grid and extremely affects the stability of the power grid, particularly in weak grids and microgrids [1]-[3].

The balance between the load and generation defines the frequency stability of the power system. The existing kinetic inertia in the rotating parts of the enormous synchronous generators and turbines plays a significant role in improving the stability of the power grid by maintaining the balance between the demand and generation. The rotating parts can maintain the generation-load balance by absorbing/releasing the excessive energy. The concept of virtual synchronous generator (VSG) has been introduced to tackle the drawbacks of conventional direct-power grid-connected

inverters. The VSG concept is a control scheme which mimics the mechanical behavior of a synchronous generator. In other words, the mechanical characteristics such as the moment of inertia and the damping parameter are implemented in the form of differential equations to behave like a synchronous generator. In this method, the difference between the reference active power and the generated active power defines the frequency of the inverter based on the swing power equation [4]-[6].

The main drawback of the VSG concept is to increase the stability of the power system by emulating a virtual inertia to absorb/generate the excessive power. Unlike the conventional grid-connected inverter which requires a phase-locked loop (PLL), the VSG control scheme does not need a PLL. The implementation of highly nonlinear PLL adds to instability of the controller, particularly during the transient. Therefore, not only the stability of the power system is improved by the concept of virtual inertia, but also removing a PLL significantly improves the performance of the VSG-based inverters. Besides, by mimicking the behavior of the synchronous generator, penetration of renewable energy resources does not change the conventional SG-based power grids [7]

The conventional VSG control scheme has two main disadvantages: (i) designed for the inductive grids, and (ii) designed based on the conventional linear controller. The first drawback of the VSG is that the system is designed for the high voltage grids, which are basically inductive grids. It means that the transmission line between the inverter and the grid is mostly inductive. Therefore, the active power and reactive power can be controlled in a decoupled approach. Consequently, the active power can be controlled by the frequency or the rotating angle, and the reactive power can be regulated by the magnitude of the inverter voltage. However, if the connection is semi-resistive or

resistive, which is the case for low-voltage grids and micro grids, the decoupled assumption is no longer valid. In other words, both the rotating angle and the magnitude of the voltage play role in controlling the active and reactive power. The reactive power is controlled by a conventional proportional integral (PI) or integral (I) controller. The conventional PI/I controller are linear controllers, which are designed to control linear system. The power system consists of various nonlinear parts such as inductors and transformer which makes the system highly nonlinear. To be able to design and implement a conventional linear controller, the nonlinear system requires to be linearized in the neighborhood of the nominal operating point. Therefore, if the operating point changes the controller parameters require to be redesigned. Consequently, conventional VSG controller are not suitable for the resistive grids or the system with varying operating point [8]-[10].

In this research three approaches are proposed to tackle the drawbacks and to improve the performance of a grid connected VSG. The first approach is the utilization of a model-free neural network predictive controller (NNPC) [11] and [12]. In this approach, the exact model and parameters of the system are not required. The model neural network can be trained to perform as an approximator for the model of the system. Besides, the NNPC is based on the model predictive control (MPC), which is a nonlinear optimal controller for a finite time horizon. Therefore, this approach tackles both drawbacks of the conventional VSG. The optimization in a finite time horizon is the limitation of this method. By increasing the optimization time period, the computation gets more time consuming. To address this limitation, a control approach based on the heuristic dynamic programming (HDP) is proposed in the second paper. The HDP is an

approximation for the optimal dynamic programming. The HDP is an adaptive critic design (ACD) technique which optimally performs as a controller in an infinite time horizon. This approach tackles both drawbacks of the conventional VSG as an adaptive nonlinear controller. Since the training procedure should be done in the entire state space, training the neural network in the HDP controller is time consuming [13] and [14]. In the third paper, a dual heuristic dynamic programming (DHP) is proposed to regulate a grid-connected inverter. To train the neural network regarding the DHP, it is sufficient to perform the exploitation in the vicinity of the optimal trajectory [15]-[18]. Therefore, this method can be trained faster and perform similar advantages of the HDP-based VSG.

PAPER

I. POWER AND FREQUENCY REGULATION OF SYNCHRONVERTERS USING A MODEL FREE NEURAL NETWORK-BASED PREDICTIVE CONTROLLER

Sepehr Saadatmand, Pourya Shamsi, and Mehdi Ferdowsi

Department of Electrical Engineering, Missouri University of Science and Technology, Rolla, MO 65409

ABSTRACT

Recent trends in the utilization of renewable and sustainable energy sources have led to an increased penetration of inertia-less power electronics-based energy resources into the electrical grid. The concept of the virtual synchronous generator (VSG) has recently been studied to overcome the drawbacks of the fast-responding inertia-less inverter by mimicking the behavior of a traditional synchronous generator. The majority of literature on VSGs assume the operation of VSGs in inductive networks; however, such control algorithms do not operate well in a more resistive network such as a low voltage distribution network. This paper introduces a new neural network–based predictive control for VSGs that is capable of operating optimally in both inductive and resistive networks by optimizing the total tracking error during transients. After the introduction of the control scheme, simulation and experimental results are provided to evaluate the effectiveness of the proposed algorithm in reducing oscillations and settling time.

1. INTRODUCTION

Integration of renewable energy sources (RESs), such as wind turbines and photovoltaic (PV) arrays, into the traditional power grid has been steadily rising. Energy produced by these resources is often injected into the power grid using Voltage Source Converters (VSC). Consequently, the penetration of power inverters is increasing rapidly. Direct power/current control through methods such as vector control is the most common approach in controlling these inverters [1]–[3].

Although direct power control is a popular approach and is easy to implement, there have been studies on how to replace it with new control schemes to overcome its drawbacks. There are two main issues with direct power controllers: (i) lack of inertia and frequency irresponsiveness and (ii) the requirement for a phase-locked loop (PLL). The frequency of conventional power grids is stabilized by the rotating mass of synchronize generators (SGs). Due to the rotating rotor/turbine, there is a large amount of angular momentum available in the grid, which compensates for sudden changes or disturbances in the power flow. Hence, the existence of kinetic inertia in traditional power systems makes the systems robust against instability. Increasing the penetration of inverter-based DGs that do not have inertia leads to vulnerability of the system against sudden variations in the power flow [4]–[7]. Additionally, the direct power control requires a PLL to measure the grid's frequency and the initial angle. PLLs dynamics can impose additional stability concerns during transients, which can lead to instability of the system [8]–[12]. To overcome the aforementioned drawbacks associated with direct power control, the virtual synchronous generator (VSG) technology has been proposed

[13]–[15]. In the VSG concept, the inverter mimics the characteristics of a synchronous generator through the implementation of a virtual inertia in its dynamic model. By feeding the power reference commands as inputs to the VSG, the frequency, phase angle, and the voltage amplitude will be generated unlike a traditional direct power/current control approach, a VSG acts similarly to a synchronous generator. This will lead to improved system robustness and will eliminate the PLL requirements [16]–[19].

Several studies have explored different aspects of VSG controllers. The fundamental component in a VSG control scheme is the standard generator swing equation. Hence, in the majority of the literature, researchers have limited their work to optimizing the swing parameters, including the virtual inertia and the damping factor. In [20], the damping parameter and the moment of inertia parameter is defined using the particle swarm optimization (PSO) algorithm to optimize the deviation in the voltage and the frequency. A fuzzy-logic technique is used in [21] to compute the virtual inertia constant. A VSG with an alternating moment of inertia is suggested in [22] to improve the oscillation damping. However, in all of these studies, the main focus is on tuning VSG parameters. There have been several methods proposed to improve the VSG's main equations. Most of the proposed VSGs are studied for high-voltage grids with inductive transmission lines, and decoupled control techniques were used for the active and the reactive power [23]. To address this drawback, a power-angle synchronization method has been studied by several authors. In this technique, the inverter is a VSC, and its output voltage is adjusted to deliver the active and the reactive power demands. In this method, the active and the reactive power equations are changed in a way to enhance the power stability. The existing study on the power-angle synchronization method is limited

to high or medium-voltage systems [24]–[27], except for [28], which has investigated low voltage networks. In [29], the grid is analyzed, and a resistive compensator is designed to ensure the decoupled control for the active and reactive power.

Distinctively, this paper focuses on low-voltage grids. A microgrid with a weak grid and RESs and local loads, such as electric vehicles, can be a good example of this type of grid. The proposed method can be used to interconnect a storage source into the grid and enhance the grid stability by applying VSG control. As mentioned previously, the transmission line in low voltage grids is mostly resistive meaning that the active/reactive equations are completely different from those of an inductive grid. The main contributions of this paper include:

1) Analyzing the power delivery equations for the VSGs in a low voltage grid.
2) Proposing a neural network–based predictive controller to optimize the power system stability and the power fluctuations in both inductive and resistive grid connections.
3) Using the proposed neural network predictive controller to improve the system robustness under severe reference changes

The proposed controller inherits both inertia properties of SGs and the fast dynamic of the power inverters.

The rest of this paper is organized as follows. Section 2 describes a brief review of frequency regulation and power control in virtual inertia–based power inverters. In Section 3, the power flow equations are presented and the difficulties of the implementation of VSGs in low voltage grids are explained. The neural network predictive controller concept is introduced in Section 4. Lastly, simulation and

experimental results are provided in Section 5 to validate the effectiveness of the proposed controller method.

2. VIRTUAL SYNCHRONOUS GENERATOR

The matching between the load and demand in a grid defines the frequency deviation. During steady state operation of the system, secondary and tertiary control methods, including the power dispatch commands, will balance the load-demand equation. During transients, the rotating kinetic inertia of SGs is the primary stabilization mechanism used to smoothen the variations in frequency. To mimic this behavior, a VSC model has to be integrated into a power inverter. In this section, a VSG model is developed that can be used for both resistive and inductive grids.

2.1. PRINCIPLE OF VSG

The controller block diagram of a grid-connected VSG is shown in Figure 1. The concept of the VSG is based on the kinetic energy of the rotor which can be expressed as

$$W = \frac{1}{2}\mathrm{J}\omega_m^2 \tag{1}$$

where W is the kinetic energy of the rotor, and J and ω_m are the rotor moment of inertia and the rotor rotational speed, respectively. By taking the derivative of both sides of (1) and adding the damping factor, the swing equation can be written as

$$P_{in} - P_{out} = \mathrm{J}\omega_m \frac{d\omega_m}{dt} - \mathrm{D} \cdot \Delta\omega_m \tag{2}$$

where $P_{in}$and P_{out} are the input and output power, respectively. The damping coefficient of the active power is represented by D. In (2), $\Delta\omega_m$ can be defined as $\Delta\omega_m = \omega_m -$

ω_{grid}, where $\omega_{grid}$is the reference frequency or the grid frequency. The virtual mechanical phase θ_m can be computed by taking the integral from $\omega_m$as

$$\theta_m = \int_0^t \omega_m \cdot \mathrm{dt} \tag{3}$$

where θ_m can be the phase control command fed to the inverter for different amplitudes of voltage. Moreover, the following equation is employed for the reactive power command as

$$E = \frac{1}{k}\int \left(Q_{ref} - Q_{out} + D_q\left(V_{ref} - V\right)\right) \tag{4}$$

where Q_{ref}, and Q_{out} represent the reactive power reference and the output reactive power, respectively. The parameters D_q and k are presenting the voltage droop coefficient of reactive power and the regulating factor of reactive power, respectively. In addition, V_{ref}, V, and E are the reference voltage amplitude, the inverter output voltage amplitude, and the amplitude of electromotive force or in the case of VSG the virtual electromotive force, respectively.

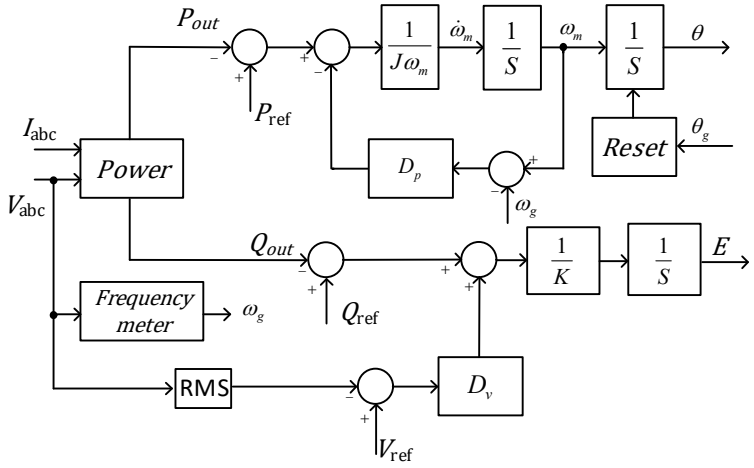

Figure 1. Block diagram of a typical grid-connected synchronverter

2.2. POWER FLOW EQUATION

The averaging model of a three-phase grid-connected inverter is shown in Figure 2. To simplify the equations and to highlight the importance of the line parameters, filtering capacitors and local loads are ignored. As shown, an inverter is connected to the grid with the per phase filtering inductance of L_f with the internal resistance of R_f where the subscript '*f*' stands for filter. The inverter is connected to the grid with a transmission line with the per phase inductance of L_l and the resistance of R_l where the subscript '*l*' stands for line. Assuming that the grid rotational frequency is ω_g, the total impedance between the inverter and the grid can be written as $Z_{eq} = R_{eq} + jX_{eq}$ where $R_{eq} = R_f + R_l$, $X_{eq} = \omega_g L_{eq}$, and $L_{eq} = L_f + L_l$; the subscript 'eq' stands for equivalent. The per phase power flow equation from inverter to the grid can be written as:

$$Q = \frac{1}{2}\left[\left(\frac{E^2}{Z_{eq}^2} - \frac{EV_g \cos\delta}{Z_{eq}^2}\right)X_{eq} - \frac{EV_g}{Z_{eq}^2}R_{eq}\sin\delta\right] \tag{5}$$

$$P = \frac{1}{2}\left[\left(\frac{E^2}{Z_{eq}^2} - \frac{EV_g \cos\delta}{Z_{eq}^2}\right)R_{eq} + \frac{EV_g}{Z_{eq}^2}X_{eq}\sin\delta\right] \tag{6}$$

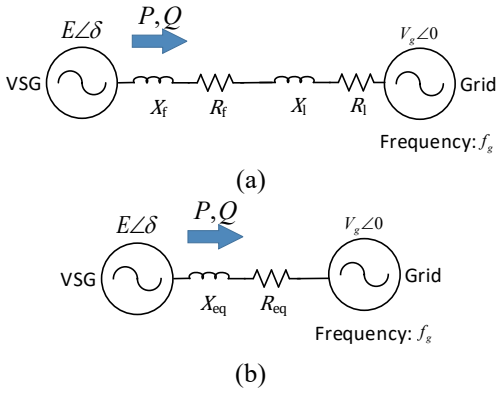

Figure 2. (a) The inverter averaging model of a grid-connected inverter (b) The equivalent circuit of the inverter averaging model of a grid-connected inverter

where P and Q are the per phase active and reactive power transferred from the inverter to the grid, respectively. In (5) and (6), E, V_g, and δ are the peak value of the phase voltage for the inverter, the peak value of the phase voltage of the grid, and δ is the phase angle between the inverter output voltage and the grid voltage. As analyzed in [30], the main idea behind the typical VSG design described in part A of this section is that in inductive grids where $X_{eq} >> R_{eq}$ the power equation (5), (6) can be rewritten as

$$Q \approx \frac{E}{2X_{eq}}(\mathrm{E} - \mathrm{V}\cos\delta) \tag{7}$$

$$P \approx \frac{EV}{2X_{eq}}\sin\delta. \tag{8}$$

Generally, the power angle δ is small; therefore, the inverter voltage E and the phase angle δ can be used as two decoupled parameters to control the active and the reactive power. However, in low-voltage grids, the inductive transmission line assumption is no longer valid. Consequently, the decoupled control strategy causes instability or long term power fluctuations. In order to overcome this issue, several solutions have been proposed to change (2) and (4) to coupled equations. The problem is that, by changing (2), the behavior of the VSG will no longer mimic an actual synchronous generator. Hence, in this paper, a new approach is proposed that tackles the voltage control problem.

3. NEURAL NETWORK PREDICTIVE CONTROL FOR VSG

In this section, a neural network–based model predictive controller (NNPC) is proposed based on the model predictive control, which provides the state-of-art output

voltage magnitude for three-phase synchronverters. This controller includes two parts: (i) the neural network representing the system model that needs to be trained off-line, and (ii) the proposed controller which is employed to compare the results with the traditional PI controller.

3.1. MODEL PREDICTIVE CONTROL (MPC)

In this paper, the state space equations are chosen to mathematically represent a system with known dynamics. The state space equations can be written as

$$\dot{X_c}(t) = \mathrm{F_c}(\mathrm{X_c}(t), U_c(t)) \tag{9}$$

$$Y_c(t) = \mathrm{G_c}(\mathrm{X_c}(t), U_c(t)) \tag{10}$$

where $\mathrm{X_c}(t)$ is the state vector, $\mathrm{U_c}(t)$ is the input vector, and $\mathrm{Y_c}(t)$ is the output vector. The derivative of state vector is a function of the state vector and the control vector, defined as $\mathrm{F_c}(\cdot)$. Moreover, the output vector is a function of the state vector and the input vector, defined as $\mathrm{G_c}(\cdot)$. The subscript 'c' in (9) and (10) stands for continuous time. Implementing the control algorithm in the micro controller forces us to model and implement the system in discontinuous criteria. In other words, (9) and (10) can be written as

$$X(k+1) = \mathrm{F}(\mathrm{X}(k), U(k)) \tag{11}$$

$$Y(k) = \mathrm{G}\big(\mathrm{X}(k), U(k)\big) \tag{12}$$

where *k* is the step number, and the time difference between each step is defined as sampling time T_s. Equations (11) and (12) state that with a known input vector and a control vector, the next state can be predicted. The main objective of the predictive

control is to define a series of control vectors, forcing the output to follow a reference trajectory as closely as possible. In traditional model predictive control (MPC), the system model or state space model of the system is used to predict the future outputs. In other words, the predictive controller defines a control policy to minimize a cost function in a specific time horizon, which is defined as:

$$J(k) = \gamma \sum_{i=1}^{N_H} [\, \|R(k+i) - Y(k+i)\|^2 + w_u \cdot \|\Delta U(k+i-1)\|^2 \,]. \qquad (13)$$

In (13), $R(\cdot)$ represents the reference vector, N_H represents the maximum horizon step time, γ is the discount factor $(0 < \gamma < 1)$ to define the importance of the future cost (for both the finite and infinite horizons), and to guarantee the convergence of the cost function for the infinite horizon. Parameter w_u is the gain vector for the control effort. There have been a great variety of solutions for the finite and infinite horizon of time both analytically and by numerical methods [31], which is out of scope of this study. In this paper, the objective is to optimize the cost function for a finite time horizon. Therefore, instead of directly dealing with the Bellman's equation (infinite time horizon), a predictive controller is applied.

3.2. NEURAL NETWORK PREDICTIVE CONTROLLER

To employ the MPC in an optimization problem, it is necessary to know the exact model of the system. However, there are many cases where the model of the system is too complicated and time consuming to implement, the exact model of the system is unknown, or the model parameters are uncertain, which leads to an ill-designed MPC. Feedforward neural networks are powerful tools to model an unknown system with

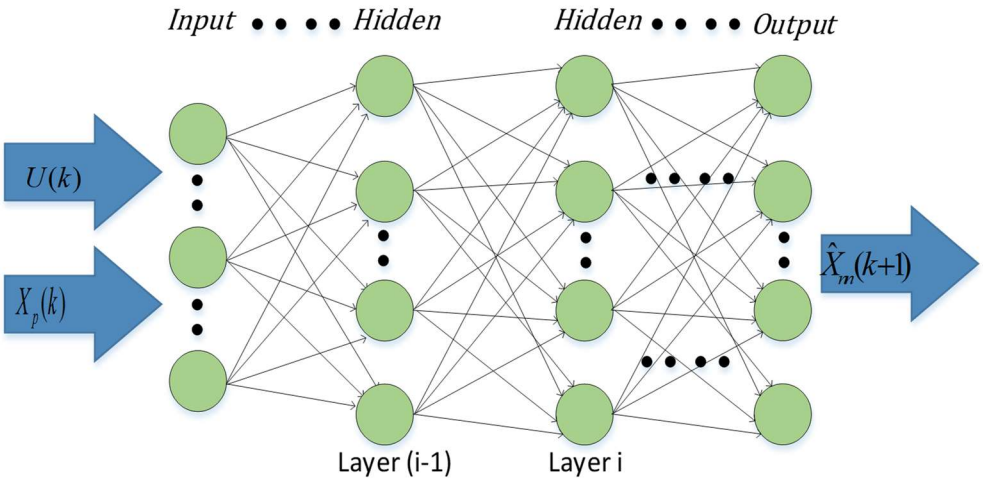

Figure 3. Multi-layer feedforward neural network

uncertain parameters. The neural network can be used as a system identifier and replace the discrete system equations (11) and (12) with an easy-to-implement method.

Figure 3 demonstrates a fully connected multilayer feedforward neural network. In this figure, $\hat{X}_{nn}$ is the next step state estimation by the neural network. A feedforward multilayer neural network is an artificial neural network with no circle between the nodes' connections on the contrary of recurrent neural networks. A multilayer feedforward neural network includes several layers in which there can be several nodes. The value of each node can be computed as

$$N_i = f(W_i \cdot N_{i-1} + b_i) \tag{14}$$

where N_i, W_i, b_i, and $f(\cdot)$ are the node value vector for the layer i, the weight matrix forming the layer i, the bias vector for layer i, and the activation function, respectively. There are several different activation functions such as sigmoid, hyperbolic tangent, and linear; however, their differences are out of the scope of this paper [32].

The neural network presenting the system model needs to be trained offline in advance. Figure 4 shows the training process where the neural network goal is to predict the next state as accurately as possible. In this procedure, random control vectors are applied to the model, and the next state values are measured. This is supervised learning; hence, we know the output for the specific input. The training procedure goal is to minimize the total error by setting the weight matrices. There have been several studies on different method to train a neural network that are out of the scope of this paper. The main goal is to sweep the system's state variables for learning the model. As shown in Figure 4, a sufficiently stabilizing control, (or in our case, a traditional PI controller to avoid large signal instability), will be applied to the plant. The neural network input includes the state vector and the control vector, and its output is an estimation of the next step state. A sample and hold unit needs to be implemented to make sure that the control signal applied to the plant does not change between two steps. Finally, after comparing

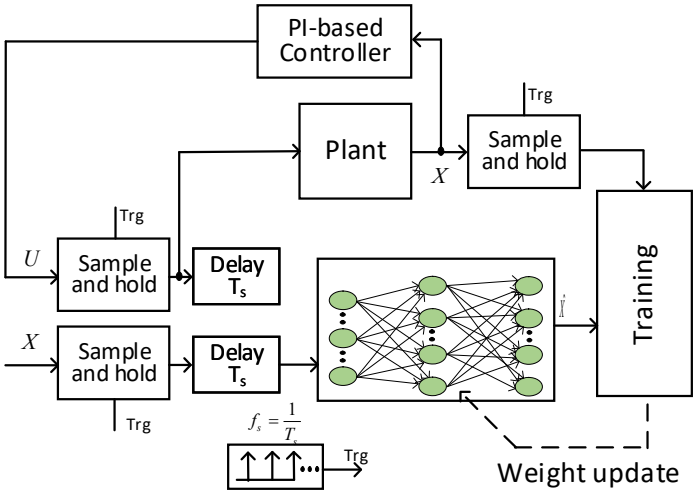

Figure 4. Training procedure for a feedforward neural network presenting the system model

the neural network estimation and the plant output, the weight matrices will be updated. Based on the definition of the neural network predictive controller, it is necessary to pretrain the neural network before implementation. If the neural network is well-trained, and the system is fixed, the NNPC can perform similar to a model predictive controller. If the system parameter changes, there are two approaches: (i) to train the neural network online, which makes the control system more complicated and timely expensive to implement, and (ii) to pretrain (offline training) the neural network offline after any changes in the system parameters [33]. After the first stage of the training, the NNPC is ready to be implemented. By replacing the system model in the traditional MPC with the presented neural network, the neural network–based model predictive control can be constructed as shown in Figure 5. As illustrated, NNPC includes two fundamental blocks: (i) the neural network block which predicts the next step state vector, and (ii) the optimization block, which minimizes the cost function defined in (13) by providing a set of control vectors. Only the first control vector is used as the optimal control, and in the

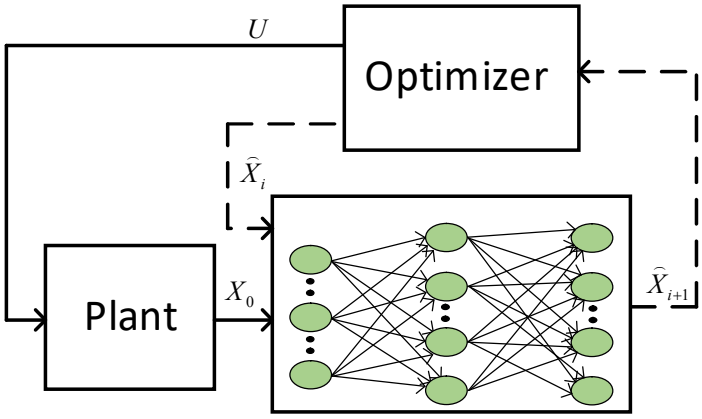

Figure 5. Neural network predictive controller block diagram

next step the entire computational procedure needs to be repeated. In this paper, all the system parameters are fixed during both simulations and experiments, therefore the neural network is pretrained once.

3.3. IMPLEMENTATION OF NNPC ON VSG

As mentioned in Section 2, the objective in this paper is to keep the swing equation unchanged. In other words, the NNPC optimizes the cost function only by controlling the voltage amplitude. To employ the NNPC algorithm, the reactive power controller in traditional VSGs, which is typically a proportional or proportional integral controller, is replaced with the proposed controller. Figure 6 shows the block diagram of the proposed controller. As shown, a fault detection and controller selection unit is also added to the traditional block diagram. Two current thresholds are defined as Tr_1 and Tr_2,

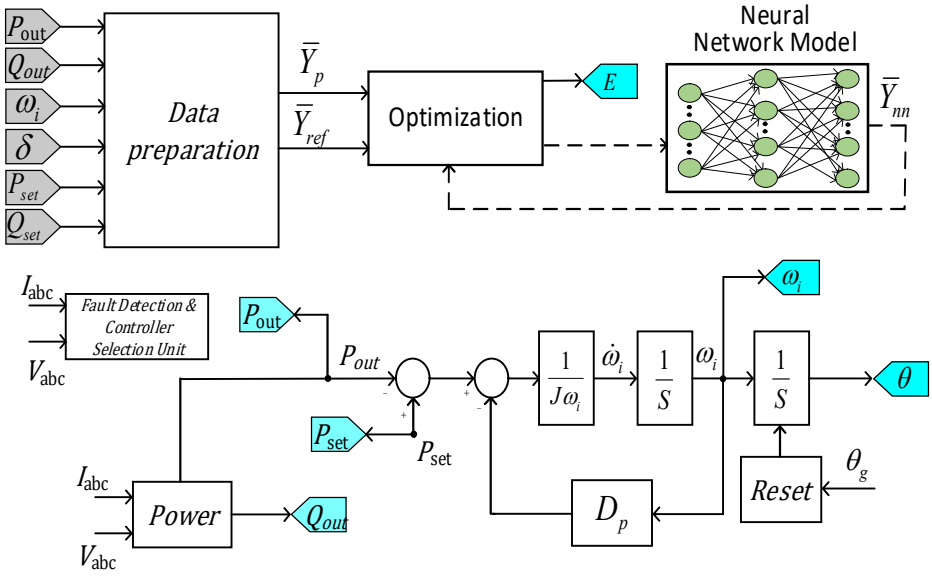

Figure 6. VSGs block diagram using NNPC

Table 1. Simulation parameters

Parameter	Value	Unit
VSG		
DC voltage	400	V
AC line voltage	110	V
AC frequency	60	Hz
Moment of inertia	0.1	Kg. m2
Frequency droop	%4	--
Inverter power rating	5	kW
Inductive line		
Filter reactance	753	mΩ
Line reactance	377	mΩ
Line resistance	10	mΩ
Resistive line		
Filter inductance	753	mΩ
Line inductance	30	mΩ
Line resistance	1000	mΩ
NNPC parameters		
Time step (Ts)	1	msec
Time horizon	10	msec
Hidden layer	2	--
Node per hidden layer	6	--

where $Tr_1 > Tr_2$. If the current goes beyond Tr_1 it activates the circuit breakers, and if the current goes beyond Tr_2, it goes back to the traditional direct current control to avoid triggering the circuit breakers.

The state vector and the control signal for the model predictive controller is defined as

$$X = \{ P, \Delta P, Q, \Delta Q, \Delta\omega, \delta \} \tag{15}$$

$$U = E \tag{16}$$

In order to model the system, a feedforward neural network is used with two hidden layers and 4 nodes at each layer. The activation function for the hidden layer is

the sigmoid function, and for the output layer, the linear activation function is used. To train the neural network, a sample and hold unit is used, which is associated with the traditional PI controller to avoid instability. The system works and 10,000 data epochs are collected. 70% of the data were used to train the network, 15% were used for the validation, and 15% were used for the testing procedure. The Levenberg- Marquardt algorithm was used as the training algorithm. The accuracy of the neural network for the simulation and experimental results are 90% and 81%, respectively. Measurement noise from sensors can reduce the accuracy in experimental results.

The cost function in the optimizer is defined as

$$J(k) = \sum_{i=1}^{10} \left\| \frac{\Delta P}{S_{base}} \right\|^2 + \left\| \frac{\Delta Q}{S_{base}} \right\|^2 + \left\| \frac{\Delta \omega}{\omega_o} \right\|^2 \quad (17)$$

where S_{base} are the base power and $\omega_o = 120\pi$. To minimize the following cost function, there is a list of choices for the control signal. As shown in (17), the optimizer objective is to minimize the cost over the next ten steps. By applying the control signal and using the neural network representing the state space model, the approximated state can be generated. Using this step and by reapplying the neural network model, following steps can also be estimated iteratively. Also, the new control strategy is selected in the neighborhood of the prior control signal to prevent large jumps in the voltage magnitude. At each control cycle, every 1 millisecond, based on the magnitude of the total error, there is a list of possible values for the inverter voltage. The value with the best results is chosen to generate the inverter voltage magnitude.

4. SIMULATION RESULTS

To evaluate the performance of the proposed controller, two scenarios are analyzed. The first scenario is when the line is inductive, and the second scenario is for the resistive transmission line. The simulation is in the MATLAB environment and the PLECS is used to simulate the electrical parts and connections. The VSG parameters, the line reactance and resistance, and the neural network features and parameters are illustrated in Table 1. Figure 7 and Figure 8 illustrate the simulation results.

4.1. INDUCTIVE TRANSMISSION LINE

As discussed in Section 2, the performance of the traditional VSGs with an inductive line connecting to the grid, is acceptable. Where the line is inductive, the

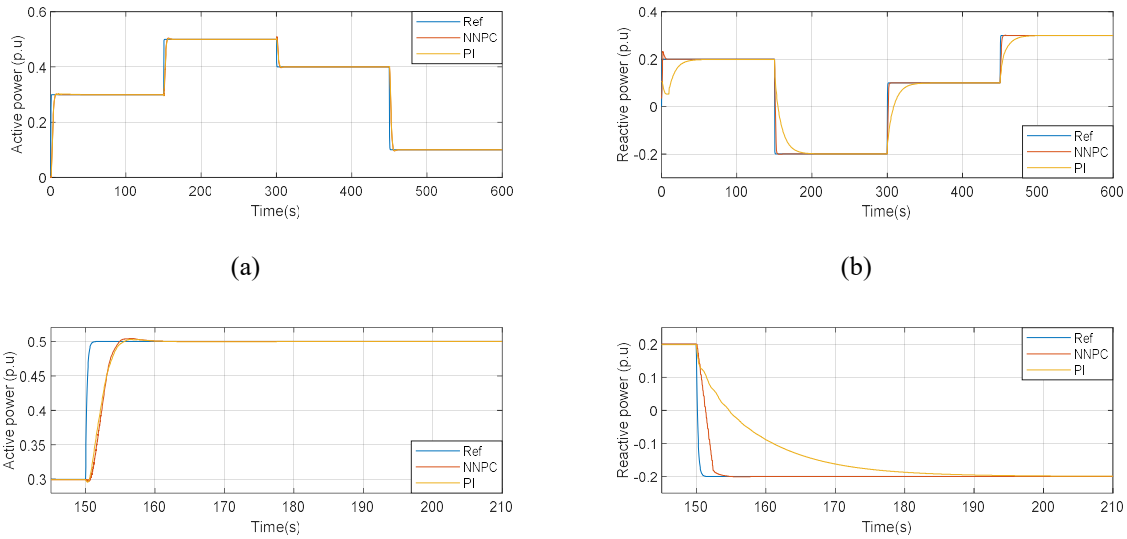

Figure 7. Comparison of the performance of NNPC VSG and traditional VSG connected to the inductive grid (a) active power, (b) reactive power, (c) active power (zoomed in), (d) reactive power (zoomed in)

relation between the active power and the power angle and the relation between the reactive power and the voltage amplitude can be considered as two decoupled control equation. Consequently, the performance of the traditional VSG is acceptable. Figure 7 compares the performance of the NNPC and the traditional PI controller. As expected, both controllers perform with good behavior in tracking the power references. However, the NNPC performs relatively better than the traditional controller, because the line is not completely inductive.

4.2. RESISTIVE TRANSMISSION LINE

In this part the performance of the NNPC for the VSG is evaluated and compared with the traditional PI-based decoupled active and reactive controller. This paper

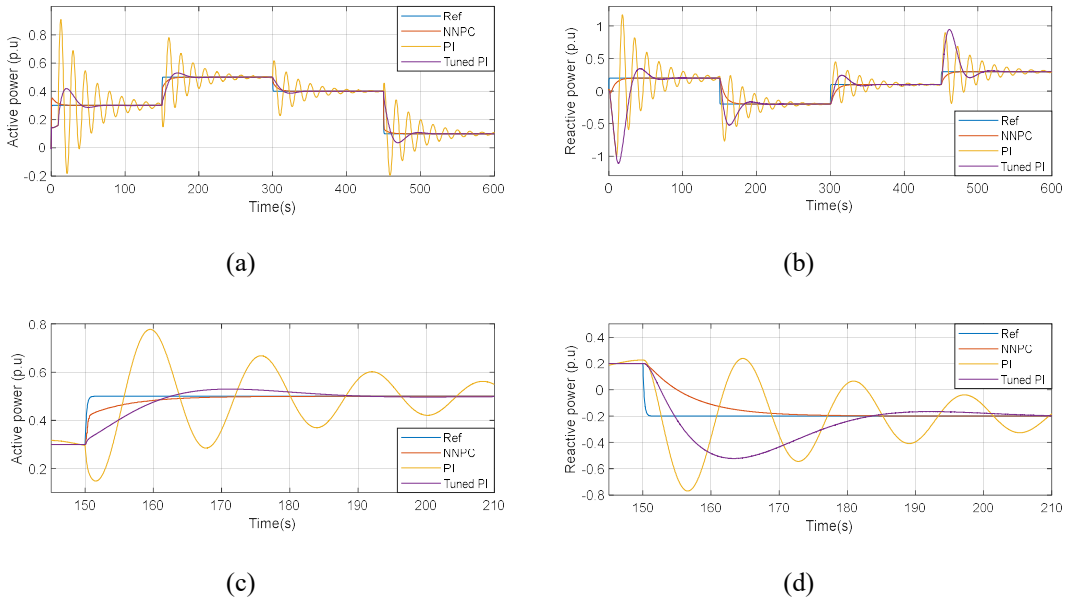

Figure 8. Comparison of the performance of NNPC VSG and traditional VSG connected to the resistive grid. (a) active power, (b) reactive power, (c) active power (zoomed in), (d) reactive power (zoomed in)

proposes NNPC for a model-free system, therefore the MPC, which needs the system model, is not implemented. In Section 2, it is mentioned that in resistive grids, the swing equation and reactive power-voltage droop equation is no longer valid. Therefore, as was expected, the traditional PI-based VSG performance is not acceptable, and there are many power swings and fluctuations that occur until it reaches the steady state. A more advanced PI-based control tuned for resistive conditions is also simulated. In this controller, both active and reactive error contribute to control the voltage. However, the portion of contribution of each one is not fixed and depends on the system parameters and hence, a large signal tuning is not possible. This method improves the performance but is not ideal and cannot guarantee the stability on the large variations of commands (particularly, large steps on the reactive power injection). On the contrary, the NNPC VSG is trained for the resistive line and adjusted itself to provide an optimum control for following the active and reactive power reference changes. Figure 8 shows the comparison between the traditional and tuned VSGs and the proposed NNPC. Figure 9

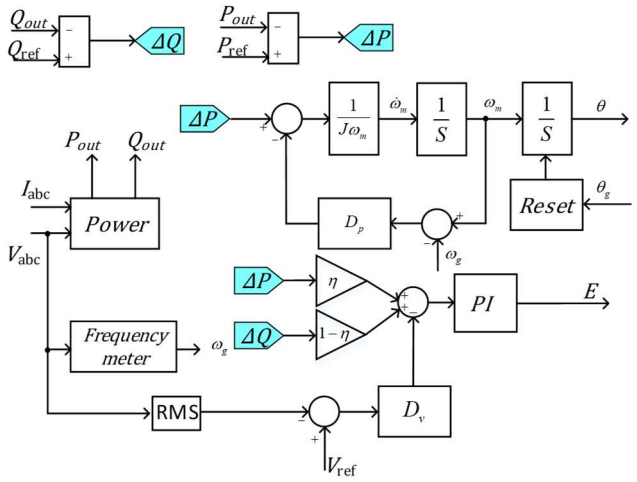

Figure 9. Block diagram of tuned PI controller for resistive grids

Table 2. PI parameters for the simulation design

Parameter	Value
Inductive grid	
K_p	.8
K_i	65
Resistive grid	
Kp	.4
K_i	30
Resistive grid (tuned)	
K_p	.7
K_i	45
η	0.6

illustrates the block diagram of the proposed tune PI controller. In this figure η is in [0,1] which defines the portion of each error in to adjust the voltage magnitude. Table 2 illustrates the controller parameter which is used for the simulation.

5. EXPERIMENTAL RESULTS

The experimental results are reported for a 1kVA laboratory prototype. The grid voltage is a three-phase with 190V/60Hz line-line voltage. The control algorithm is implemented in Texas instrument signal processor TMS320F28377. The direct current control, the traditional VSG, and the NNPC VSG are implemented to regulate the active and reactive power and the frequency. The prototype is shown in Figure 10.

The first step of the procedure is to connect the inverter to the grid. There are several methods to connect the inverter to the grid; however, in this paper, a PLL with a low-pass filter is used to detect the grid rotational angle. Moreover, the zero crossing

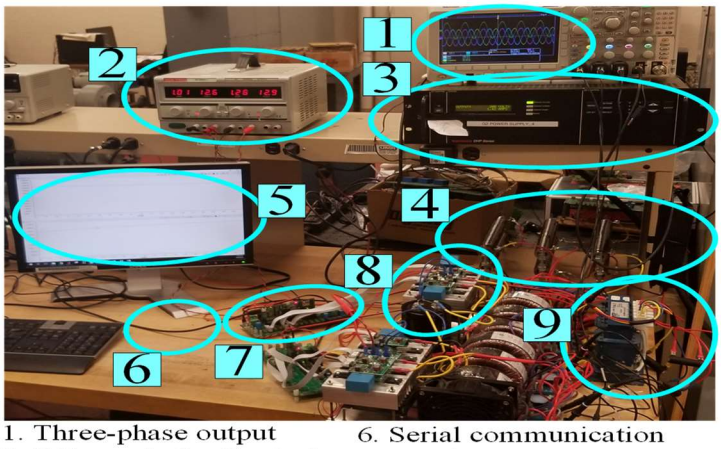

Figure 10. Three-phase grid-connected inverter test bed

method is available to avoid using the PLL. After connecting the inverter to the grid, it works under the traditional VSG control scheme until the neural network is trained.

At first, the neural network presenting the system model needs to be trained. To collect the data, the inverter functions under several random and bounded active and reactive references. The state information was sent to the computer to be stored. After collecting 10 million data samples to cover a vast operating domain, 10,000 of the samples were selected randomly to train the neural network to avoid overfitting. In order to train the neural network, MATLAB was used with a similar setting for the neural network. By training the weight matrices and the bias vectors, the neural network is formed and implemented into the microprocessor

As mentioned previously, the objective of this paper is to improve the performance of the VSG in resistive grid connections. Furthermore, the inductive case is not analyzed for the experimental results, and thus it was simulated and investigated in

Table 3. Experimental testbed parameters

Parameter	Value	Unit
VSG		
DC voltage	400	V
AC line voltage	110	V
AC frequency	60	Hz
Moment of inertia	0.5	Kg. m2
Frequency droop	%4	--
Inverter power rating	1	kW
Line Parameters		
Filter reactance	900	mΩ
Line reactance	150	mΩ
Line resistance	1800	mΩ

Table 4. PI parameters

Parameter	Value
Resistive grid	
K_p	0.19
K_i	40

Section 3. Table 3 illustrates the prototype data and parameters. Table 4 illustrates the PI parameters.

The optimization procedure for the short time horizon can be done in the DSP. However, in this case the optimization is done by MATLAB.

Figure 11 shows the performance of the VSG in regards to the active power reference changing. In this experiment, the reactive reference power is fixed within 0.1 p.u, and the active power reference changes four times in the following sequence {0.05 0.1 0.2 0.4 0.6} p.u. In this figure, the top signal is the output reactive power where 2.5V is set to zero VAR, 5V is set to 500VAR, and 0V is set to -500VAR. Moreover, the bottom signal is the active power output where 5V is 1000W and 0V is 0W. Figure 11 (a) shows the response of the traditional PI-based VSG, and the active power changing and

the magnified version is illustrated in (b). As shown, the traditional response causes oscillations and relatively large overshoots. The NNPC performance in regards to changing active power references is shown in (c), and the magnified version is shown in (d). Needless to say, the NNPC demonstrates a better response compared to the traditional VSG and significantly improves the overshoot rate and the oscillation problem. The line voltage and the line current are also shown in Figure 12, which illustrates the changes in the voltage and in the current with regards to the change in power.

The experiment is repeated with changes in the reactive power reference. Similar to Figure 11, in Figure 13, the top and bottom signals show the reactive and the active

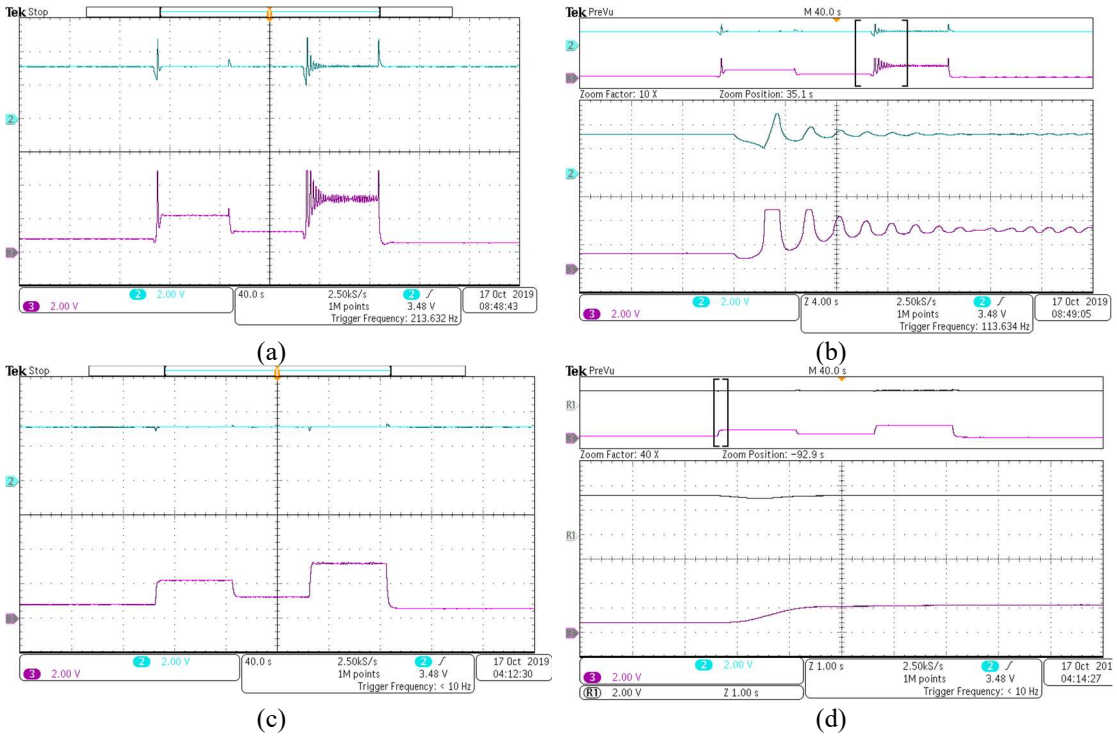

Figure 11. Injected active and reactive power from a three-phase grid connected synchronousverter facing active power reference changes (a) traditional VSG, (b) magnified response for traditional VSG, (c) NNPC (d) magnified NNPC

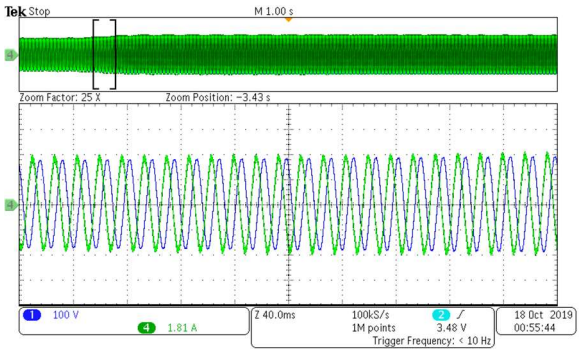

Figure 12. The phase output voltage and the line current of synchronousverter after the low-pass filter

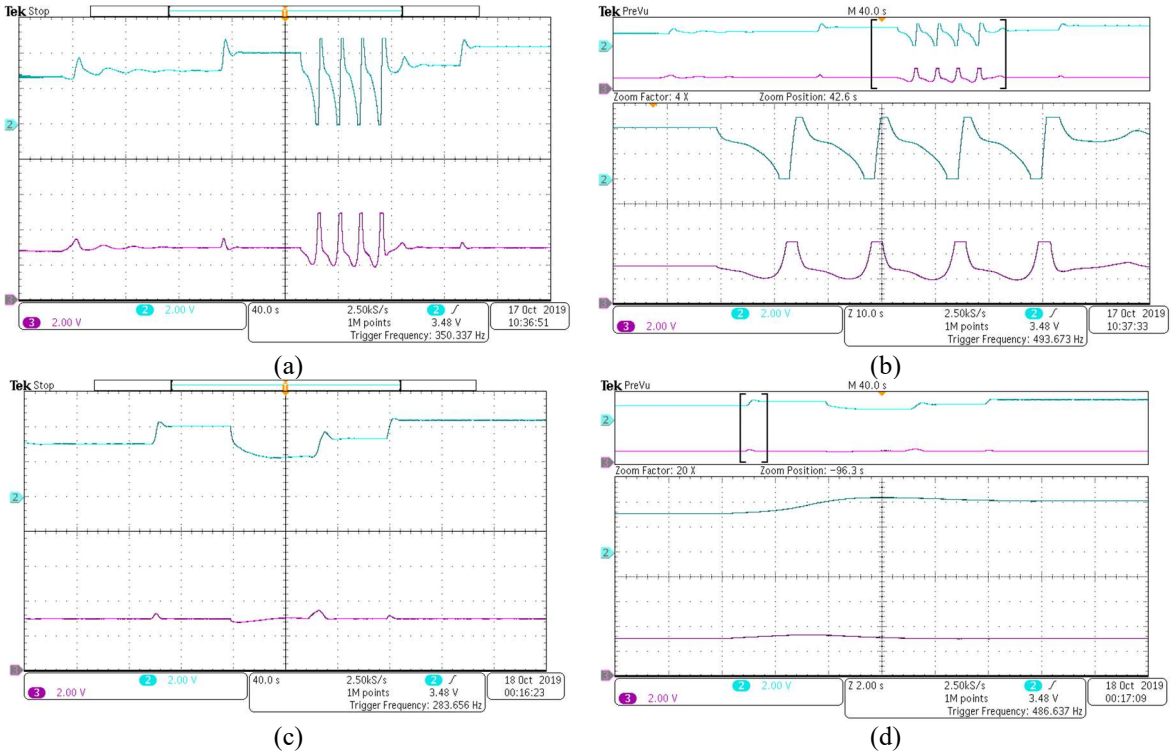

Figure 13. Injected active and reactive power from a three-phase grid connected synchronverter facing reactive power reference changes (a) traditional VSG, (b) magnified response for traditional VSG, (c) NNPC (d) magnified NNPC

output, respectively. As shown in Figure 13, the active power is fixed on 0.1 p.u. The reactive power changes in sequence of {0.1, 0.4, -0.1, 0.2, 0.5} p.u. Figure 13(a) illustrates that the PI-based VSG controller responds with large overshoots or even

becomes unstable. In this figure, the active power is shown with a dc output on prob 1, where 1000W is shown by 5v and -1000W is shown by 0v; moreover, the reactive power is measured through a voltage signal where 700VA is 5v and -700 VA is 0v. On the other hand, as expected from the mathematical point of view and the simulation results, the proposed NNPC performs much better than the traditional VSG. The spikes in active and reactive power can be minimized if the swing equation changes as well; nevertheless, the assumption of this paper is to keep the swing equation part of the VSG model unchanged.

6. CONCLUSION

In this paper, a new neural network predictive control method was presented to optimize the performance of VSGs in non-inductive grids. This controller has two main blocks: (i) the neural network block, which models the system, and (ii), the optimizer, which optimize the total error during the transient time. The traditional VSGs are based on decoupled control methods for the active-phase angle and the reactive power-voltage, which is not the case in non-inductive grids. The proposed controller sets the inverter output voltage to minimize the active and reactive errors and the frequency deviation. A well-trained NNPC for VSG can improve the VSG's performance in inductive grids, but especially in non-inductive grids. The simulations and experimental results illustrate the enhancement in tracking the power references.

REFERENCES

[1] F. Blaabjerg, R. Teodorescu, M. Liserre, and A. V. Timbus, "Overview of control and grid synchronization for distributed power generation systems," *IEEE Trans. Ind. Electron*., vol. 53, no. 5, pp. 1398–1409, Oct. 2006.

[2] J. M. Guerrero, J. C. Vasquez, J. Matas, L. G. de Vicu˜na, and M. Castilla, "Hierarchical control of droop-controlledAC andDCmicrogrids—A general approach toward standardization," *IEEE Trans. Ind. Electron*., vol. 58, no. 1, pp. 158–172, Jan. 2011.

[3] H. Bevrani, M. Feizi, and S. Ataee, "Robust frequency control in an islanded microgrid: Hinf and μ-synthesis approaches," *IEEE Trans. smart Grid*, vol. 7, no. 2, pp. 706–717, Jul. 2015.

[4] E. Rakhshani, D. Remon, A. Cantarellas, and P. Rodriguez, ``Analysis of derivative control based virtual inertia in multi-area high-voltage direct current interconnected power systems," *IET Generat., Trans. Distrib*., vol. 10, no. 6, pp. 1458_1469, May 2016.

[5] D. Li, Q. Zhu, S. Lin, and X. Y. Bian, ``A self-adaptive inertia and damping combination control of VSG to support frequency stability," *IEEE Trans. Energy Convers*., vol. 32, no. 1, pp. 397_398, Mar. 2016.

[6] H. Jafarian, M. Biglarbegian, and B. Parkhideh, "Controller robustness analysis of grid-tied AC-stacked PV inverter system considering manufacturing inaccuracies," *IEEE Applied Power Electronics Conference and Exposition (APEC)*, 2017.

[7] J. Zhu, C. D. Booth, G. P. Adam, A. J. Roscoe, and C. G. Bright, "Inertia emulation control strategy for VSC-HVDC transmission systems," *IEEE Trans. Power Syst*., vol. 28, no. 2, pp. 1277–1287, May 2013.

[8] M. Ramezani, S. Golestan, S. Li, and J. M. Guerrero, "A simple approach to enhance the performance of complex-coefficient filter-based PLL in grid-connected applications," *IEEE Transactions on Industrial Electronics*, vol. 65, no. 6, pp. 5081–5085, 2018.

[9] D. Dong, B. Wen, D. Boroyevich, P. Mattavelli, and Y. Xue, "Analysis of phase-locked loop low frequency stability in three-phase grid-connected power converters considering impedance interactions," *IEEE Trans. Ind. Electron*., vol. 62, no. 1, pp. 310–321, Jan. 2015.

[10] S. Golestan, M. Monfared, and F. D. Freijedo, "Design-oriented study of advanced synchronous reference frame phase-locked loops," *IEEE rans. Power Electron*., vol. 28, no. 2, pp. 765–778, Feb. 2013.

[11] H. X. Nguyen, T. N.-C. Tran, J. W. Park, and J. W. Jeon, "An adaptive linear-neuron-based third-order PLL to improve the accuracy of absolute magnetic encoders," *IEEE Transactions on Industrial Electronics*, vol. 66, no. 6, pp. 4639–4649, 2019.

[12] Y. Hirase, K. Abe, K. Sugimoto, and Y. Shindo, "A grid connected inverter with virtual synchronous generatormodel of algebraic type," IEE J. Trans. Power Energy, vol. 132, no. 4, pp. 371–380, Jan. 2012.

[13] Y. Ma, W. Cao, L. Yang, F. F. Wang, and L. M. Tolbert, "Virtual synchronous generator control of full converter wind turbines with short-term energy storage," *IEEE Transactions on Industrial Electronics*, vol. 64, no. 11, pp. 8821–8831, 2017.

[14] Q. Zhong, P. Nguyen, Z. Ma, andW. Sheng, "Self-synchronised synchronverters: Inverters without a dedicated synchronisation unit," *IEEE Trans. Power Electron*, vol. 29, no. 2, pp. 617–630, Feb. 2014.

[15] S. A. Khajehoddin, M. Karimi-Ghartemani, and M. Ebrahimi, "Grid-supporting inverters with improved dynamics," *IEEE Transactions on Industrial Electronics*, vol. 66, no. 5, pp. 3655–3667, 2019.

[16] Q. Zhong and G. Weiss, "Synchronverters: Inverters that mimic synchronous generators," *IEEE Trans. Ind. Electron*, vol. 58, no. 4, pp. 1259– 1267, Apr. 2011.

[17] T. Shintai, Y. Miura, and T. Ise, "Oscillation damping of a distributed generator using a virtual synchronous generator," *IEEE Trans. Power Del*., vol. 29, no. 2, pp. 668–676, Apr. 2014.

[18] V. Karapanos, S. de Haan, and K. Zwetsloot, "Real time simulation of a power system with VSG hardware in the loop," in Proc. *37th Annu. Conf. IEEE Ind*. Electron. Soc. (IECON), Nov. 2011, pp. 3748–3754.

[19] Q.-C. Zhong, P.-L.Nguyen, Z. Ma, andW. Sheng, "Self-synchronized synchronverters: Inverters without a dedicated synchronization unit," *IEEE Trans. Power Electron*., vol. 29, no. 2, pp. 617–630, 2014.

[20] B. Rathore, S. Chakrabarti, and S. Anand, "Frequency response improvement in microgrid using optimized VSG control," in *Proc. Nat. Power Sys. Conf*., Bhubaneswar, India, 2016, pp. 1–6.

[21] Y. Hu,W.Wei, Y. Peng, and J. Lei, "Fuzzy virtual inertia control for virtual synchronous generator," in Proc. 35th Chin. *Control Conf*., Chengdu, China, 2016, pp. 8523–8527.

[22] J. Alipoor, Y. Miura, and T. Ise, "Power System Stabilization Using Virtual Synchronous Generator With Alternating Moment of Inertia," *IEEE Journal of Emerging and Selected Topics in Power Electronics*, vol. 3, no. 2, pp. 451–458, 2015.

[23] L. Zhang, L. Harnefors, and H.-P. Nee, "Power-synchronization control of grid-connected voltage-source converters," *IEEE Trans. Power Syst*., vol. 25, no. 2, pp. 809–820, May 2010.

[24] M. Zhixin, F. Lingling, D. Osborn, and S. Yuvarajan, "Wind farms with HVDC delivery in inertial response and primary frequency control," *IEEE Trans. Energy Convers*., vol. 25, no. 4, pp. 1171–1178, Dec. 2010.

[25] M. Ashabani and Y. A. R. I. Mohamed, "Novel comprehensive control framework for incorporating VSCs to smart power grids using idirectional synchronous-VSC," *IEEE Trans. Power Syst*., vol. 29, no. 2, pp. 943–957, Mar. 2014.

[26] M. Ashabani andY. A.-R. I. Mohamed, "Integrating VSCs to weak grids by nonlinear power damping controller with self-synchronization capability," *IEEE Trans. Power Syst*., vol. 29, no. 2, pp. 805–814, Mar. 2014.

[27] L. Zhang, L. Harnefors, and H.-P. Nee, "Analysis of stability limitations of a VSC–HVDC link using power-synchronization control," *IEEE rans. Power Syst.*, vol. 26, no. 3, pp. 1326–1336, Aug. 2011.

[28] S. Mukherjee, V. R. Chowdhury, P. Shamsi, and M. Ferdowsi, "Power-angle synchronization for grid-connected converter with fault ride-through capability for low-voltage grids," *IEEE Transactions on Energy Conversion*, 2018.

[29] L. Zhang, L. Harnefors, and H.-P. Nee, "Power-synchronization control of grid-connected voltage-source converters," *IEEE Trans. Power Syst.*, vol. 25, no. 2, pp. 809–820, May 2010.

[30] M. Ashabani andY. A.-R. I. Mohamed, "Integrating VSCs to weak grids by nonlinear power damping controller with self-synchronization capability," *IEEE Trans. Power Syst.*, vol. 29, no. 2, pp. 805–814, Mar. 2014.

[31] M. Ashabani and Y. A. R. I. Mohamed, "Novel comprehensive control framework for incorporating VSCs to smart power grids using bidirectional synchronous-VSC," *IEEE Trans. Power Syst.*, vol. 29, no. 2, pp. 943–957, Mar. 2014.

[32] A. Jain, J. Mao, and K. Mohiuddin, "Artificial neural networks: a tutorial," *Computer*, vol. 29, no. 3, pp. 31–44, 1996.

[33] E. Corwin, A. Logar, and W. Oldham, "An iterative method for training multilayer networks with threshold functions," IEEE Transactions on Neural Networks, vol. 5, no. 3, pp. 507–508, 1994.

II. ADAPTIVE CRITIC DESIGN-BASED REINFORCEMENT LEARNING APPROACH IN CONTROLLING VIRTUAL INERTIA-BASED GRID-CONNECTED INVERTERS

Sepehr Saadatmand, Pourya Shamsi, and Mehdi Ferdowsi

Department of Electrical Engineering, Missouri University of Science and Technology, Rolla, MO 65409

ABSTRACT

In this paper, an adaptive critic design (ACD) approach is proposed to control the phase and voltage of a grid-connected virtual synchronous generator (VSG). The penetration of fast responding inertia-less power converters significantly affect the stability of the power system, especially weak systems such as micro grids. The concept of virtual inertia addresses this concern by virtually emulating the behavior of a synchronous generator. However, the conventional VSG is designed based on two conditions: (i) fixed operating point and (ii) inductive grid connections. The performance of VSGs in low-voltage semi-resistive microgrids is far from optimal. To overcome the aforementioned concerns, a heuristic dynamic programing (HDP) approach is proposed to optimally control grid-connected VSGs. The neural-network-based inherence of the HDP enables the proposed technique to adapt to any impedance angle. The HDP controller includes two subnetworks: (i) the action network that controls the system optimally and (ii) the critic network, which evaluates the effectiveness of the action network. The simulation and experimental results are provided to evaluate the effectiveness of the proposed technique. As shown, the HDP-based approach illustrates a

better performance in comparison with the conventional PI-based VSG in various operating conditions.

1. INTRODUCTION

The significance of environmental and energy crises has become highlighted in recent decades; therefore, distributed generations (DGs) have attracted a great variety of considerations in modern power systems [1,2]. The environmentally friendly and sustainability characteristics of renewable energy resources (RESs), such as photovoltaics [3] and wind turbines, have caused a rising increase in the penetration of RESs into the power grid. Three-phase inverters are the most common technique used to connect DGs into the power grid. The accelerating growth in the integration of RESs into the power grid drastically changes the conventional power grid [4]. The stored kinetic energy in the enormous rotating parts of synchronous generators plays a vital role in stabilizing the power system. The balance between the demand and generation is the main factor in maintaining the frequency stability. The unbalanced condition between the generation and demand leads to voltage and frequency fluctuations. These fluctuations can result in system instability and trigger the protection systems. The existing kinetic inertia in traditional power systems can maintain the balance between the generation and the demand by releasing or absorbing the difference between the generation and demand. The inertia-less and fast-responding characteristics of power electronics inverters drastically reduce the power system stability and robustness, especially in weak grids such as microgrids [5–7].

The existing kinetic inertia in traditional power systems inspired researchers to tackle these drawbacks by emulating the mechanical behavior of synchronous generators into the control block of grid-connected inverters. A great variety of studies have been done to introduce a general solution to overcome the inertia-less characteristic of inverter-based DGs. Eventually, the concept of the virtual synchronous machine/generator (VSM/VSG) was introduced to improve the system inertia, output impedance, and resiliency of the power system [8–10]. The VSG concept is based on the behavior of synchronous generators and the so-called swing equation that enables the inverter to store/release energy during transients to maintain the balance between the generation and demand. To elaborate the importance of the virtual inertia concept, a comparison between the traditional droop control and VSG technique has been proposed in [11] that highlights the positive sides of the virtual inertia-based controller. The authors in [12] have illustrated that by considering the dynamics of the line and converter, the virtual inertia parameters are constrained by the stability considerations. The small-signal angular stability of a power system is examined in [13] when it is connected to VSGs. In order to damp the power and frequency perturbations, a fuzzy controller approach is implemented to regulate grid-connected VSGs [14]. An extended virtual synchronous generator concept is proposed in [15], where an H∞ control method is used to tune the VSG parameters. The characteristics of frequency response of the alternating current is analyzed in [16] to enhance the performance of VSGs. The authors in [17] have enhanced the performance of multi-VSG grids by focusing on the center of inertia frequency during the short circuit. In all of the proposed techniques, the system's model is required to design the controller. Changes in the parameters of the system affect

the behavior of the controller. Therefore, several studies have tackled this drawback by proposing adaptive control techniques. An adaptive virtual inertia control scheme using the bang-bang control strategy is proposed in [18] to improve the stability of the system. A neural network predictive VSG [19], self-tuning VSG in photovoltaic-diesel microgrids [20], and an adaptive VSG based on a small-signal model [21] are also proposed. However, all of these methods lack the implementation of a model-free, adaptive, optimal control. The reinforcement learning techniques are powerful tools to address these concerns and they are widely used in various applications. For example, an action-critic network is proposed in [22] to learn the optimal policy in internet of vehicles, by considering the unknown environment's dynamics. A deep post-decision state (PDS)-based experience replay and transfer (PDS-ERT) have been implemented in [23] as a reinforcement learning technique to learn the optimal policy in a heterogeneous network. To tackle the aforementioned drawbacks in regulating VSGs, two control approaches based on reinforcement learning have been proposed in [21] and [22] to regulate a grid-connected VSG. However, none of those provides the implementation of online training and the current protection in an experimental prototype.

The main contribution of this paper is to propose a heuristic dynamic programming control technique to improve the power and frequency stability of grid-connected inverters. This paper

• Presents a neural-network-based adaptive controller, which can adjust the controller setting based on the system's parameters.

• Provides online training to prevent tuning of the controller's parameters by the operator.

• Describes an optimal control to regulate the power and the frequency of a grid-connected inverter facing resistive grid.

The controller is designed to be applicable to both virtual synchronous generators and synchronous generators. The proposed reinforcement technique improves the performance of the VSG by considering the transmission line parameters and operating points. Although the virtual parameters such as virtual moment of inertia, or the droop coefficient can be set by the reinforcement technique, but in this paper, it is assumed that these parameters are predefined by the operator which enables this technique to be compatible with synchronous generators as well.

The rest of the paper is organized as follows. Section 2 explains the concept of virtual synchronous generators and highlights the weakness of the conventional VSG controllers. The heuristic dynamic programing concept, design procedure, and training algorithm are discussed in Section 3. In section 4, the proposed HDP-based VSG is proposed, and the simulation results are provided to evaluate the effectiveness of the proposed technique. The implementation procedure including the prototype's parameters are explained in Section 5, and the experimental results are illustrated to evaluate the effectiveness of the proposed technique in a laboratory prototype.

2. GRID-CONNECTED VIRTUAL SYNCHRONOUS GENERATOR

As explained in Section 1, the performance of virtual-inertia-based inverters depends on the system's parameters. To address this concern, the concept of VSG is

explained, and the effect of grid types on the VSG performances is discussed in this section.

2.1. VIRTUAL SYNCHRONOUS GENERATOR

A significant concern about the virtual-inertia-based inverters is the availability of the energy storage to perform as a source for the virtual inertia. Therefore, it is assumed that a regular dc source is connected to the dc side. Figure 1 illustrates the block diagram of conventional VSGs. In this figure, the resistance and reactance of the grid line are R_L and X_L, respectively. The filter reactance is X_F. The swing equation is the main component of any virtual-inertia-based inverter, which can be written as

$$P_{in} - P_{out} = J\omega_i\left(\frac{d\omega_i}{dt}\right) + D\Delta\omega \tag{1}$$

where the angular frequency of the virtual rotor is defined as ω_i, and the angular frequency deviation is defined as $\Delta\omega = \omega_i - \omega_g$. In this expression, parameter ω_g is the reference angular frequency when the inverter functions in a standalone mode or the grid angular frequency when it operates in a grid-connected mode. The virtual moment of inertia and the droop coefficient are defined as J and D. The electric output power and the input power are noted as P_{in} and P_{out}, respectively.

In order to drive an inverter two parameters are required: (i) the peak/RMS value (E) of the inverter voltage and the inverter phase (δ) with respect to a reference, (the grid phase is assumed as the reference). A power meter unit is used to convert the inverter three-phase current and voltage to the output electric active/reactive power. By implementing all the parameters in (1), the frequency deviation can be found. By taking the integral of the frequency deviation, the inverter phase can be computed as:

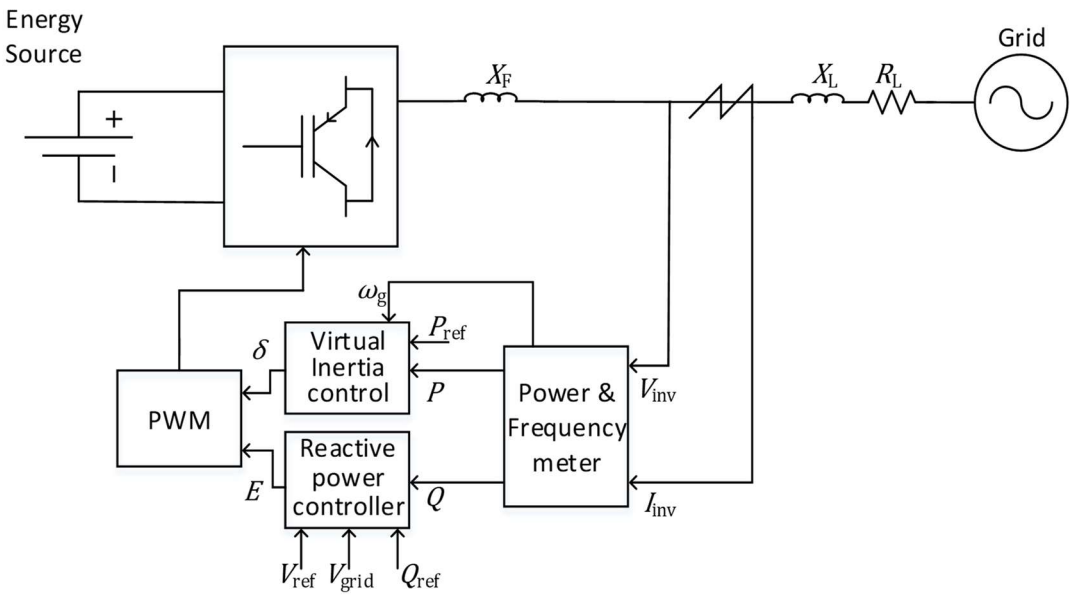

Figure 1. The block diagram of the traditional VSGs

$$\delta = \int \Delta\omega \cdot dt. \tag{2}$$

Voltage-droop-based reactive power compensator is the most common approach in regulating the inverter voltage in inductive grid. Therefore, the inverter voltage can be computed as:

$$E = \frac{1}{K_i}\int \Delta Q \cdot dt - D_v \Delta V \tag{3}$$

where D_v and K_i are the voltage droop and the integrator coefficient, respectively. The error signals for the reactive power and the inverter voltage are defined as $\Delta Q = Q_{ref} - Q_e$ and $\Delta V = V_{ref} - V_i$, respectively. The notation V_{ref} and V_i are the inverter reference voltage and the inverter output voltage, respectively. The block diagram of the active-power-phase and reactive-power-voltage of a VSG are shown in Figure 2.

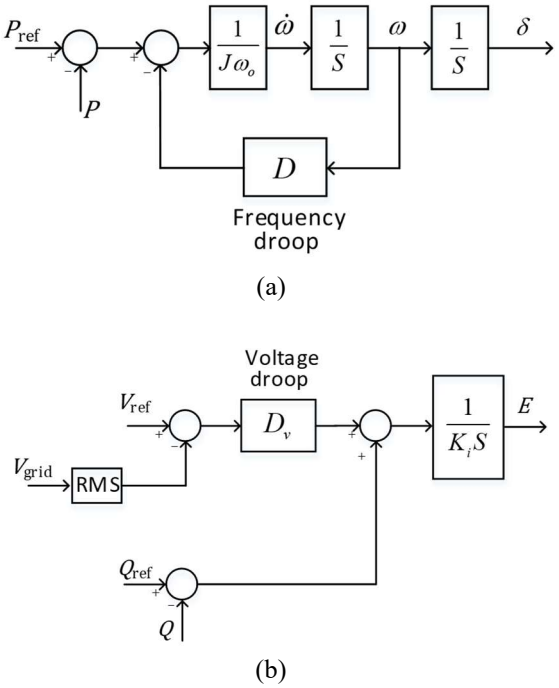

Figure 2. The block diagram of the decoupled approach for VSGs. (a) the block diagram of active power-frequency, (b) the block diagram of reactive

2.2. POWER ANGLE AND POWER FLOW EQUATIONS

A simplified circuit diagram of a grid-tied VSG based on the average model is depicted in Figure 3. In this figure, the total reactance including filter and line is defined by $X_{eq} = X_F + X_L$. The line equivalent resistance is presented by $R_{eq} = R_L$. Lastly, the

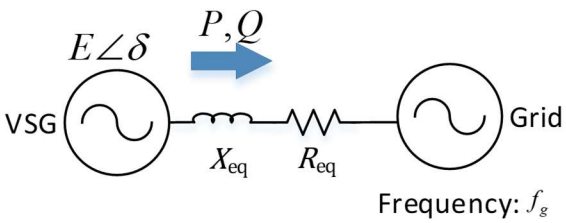

Figure 3. The simplified circuit diagram of a grid-tied VSG based on the average model

equivalent impedance can be presented by $Z_{eq} = jX_{eq} + R_{eq}$. The delivered active and reactive power from inverter to the grid can be computed as:

$$P = \frac{1}{2}\left[\left(\frac{E^2}{Z_{eq}^2} - \frac{EV\cos\delta}{Z_{eq}^2}\right)R_{eq} + \frac{EV}{Z_{eq}^2}X_{eq}\sin\delta\right] \quad (4)$$

$$Q = \frac{1}{2}\left[\left(\frac{E^2}{Z_{eq}^2} - \frac{EV\cos\delta}{Z_{eq}^2}\right)X_{eq} - \frac{EV}{Z_{eq}^2}R_{eq}\sin\delta\right] \quad (5)$$

where E, V, δ, P and Q are the peak value of the inverter voltage, the peak value of the grid voltage, the inverter power angle, the active power delivered from the inverter into the grid, and the reactive power delivered from the inverter into the grid, respectively. For an inductive equivalent impedance (i.e. $X_{eq} \gg R_{eq}$ as in [7,26]) the active and reactive power

$$P \approx \frac{EV}{2X_{eq}}\sin\delta \quad (6)$$

$$P \approx \frac{EV}{2X_{eq}}\sin\delta \quad (7)$$

can be estimated as:

Considering the fact that the power angle is typically small, by approximating $\sin\delta$ and $\cos\delta$, the power equations can be rewritten as follows:

$$P \approx \frac{EV}{2X_{eq}}\delta \quad (8)$$

$$Q \approx \frac{E}{2X_{eq}}(\mathrm{E} - \mathrm{V}) \quad (9)$$

Equations (8) and (9) validate the decoupled assumption in inductive grids. In other words, the reactive and active power are proportional to the voltage magnitude and the power angle of the inverter, respectively. Based on (8) and (9) the performance of the traditional VSG is acceptable in inductive grid connections; nevertheless, in noninductive

grids, such as low-voltage grids, this assumption is no longer valid. It means both the voltage magnitude and the phase angle contribute in generating the reactive power. This issue changes the control problem from a decoupled single input single output (SISO) into a coupled multiple input multiple output (MIMO). The conventional linear controllers are not suitable for MIMO cases. Although there are other methods, such as the model predictive control (MPC) or nonlinear control techniques that are able to deal with MIMO, but the accurate values of system model parameters are required to guarantee an ideal performance. This is not always the case in power system with several uncertainties and unknown parameters, such as nonlinear behaviors (e.g. transformer saturation), missing system parameters, or line impedance changes. To overcome these concerns, an adaptive critic design approach based on the approximate dynamic programming is proposed in this paper. The proposed technique allows parameters to be adjusted to guarantee an optimal solution for a grid-connected VSG.

3. HEURISTIC DYNAMIC PROGRAMING

Conventional VSGs are based on a conventional linear controller such as integral/proportional-integral controllers, which limits the performance of a VSG in several aspects. First, the conventional controllers require redesigning or tuning after any significant change in system parameters. This process can be done online, or it can be done offline by an experienced designer. Secondly, conventional linear controllers are designed for linear systems. Grid-connected VSGs are highly nonlinear, hence the linearized model in the vicinity of their nominal operating point is used. In other words,

operating in conditions far from the nominal operating point changes the linearized model, and it affects the performance of the linear controller. Lastly, as discussed in Section 2, linear controllers are designed for the SISO systems and non-inductive grids, and where the system is MIMO, the proposed integral-controller-based VSG is infeasible. Therefore, an adaptive critic design (ACD) approach is proposed in this paper to address the aforementioned disadvantages.

To cope with nonlinear noisy environment and uncertain systems, neurocontrol adaptive critic designs are ideal choices. The concept of ACD was introduced in [27] as a new optimization technique stimulated by the reinforcement learning and the approximate/adaptive dynamic programing (ADP).

Typical ACDs include two subnetworks: the critic neural network and the action neural network. The goal of the critic network is to provide the required feedback signal to train the action network. Different feedback signals distinguish between different types of ACDs.

The heuristic dynamic programming (HDP) is the most straightforward ACDs. Figure 4 shows the block diagram of an HDP controller. The main objective of critic networks is to approximate the cumulative discounted utility function (known as the cost-to-go function), which in dynamic programing is known as the Bellman's equation. The action network generates the control signal and feeds it to the system and to the critic network. The state vector and the control signal feed the critic network when its goal is to estimate the cost-to-go function. In Figure 5, the dashed lines illustrate the corresponding error signal for the learning procedure of the action and the critic neural network.

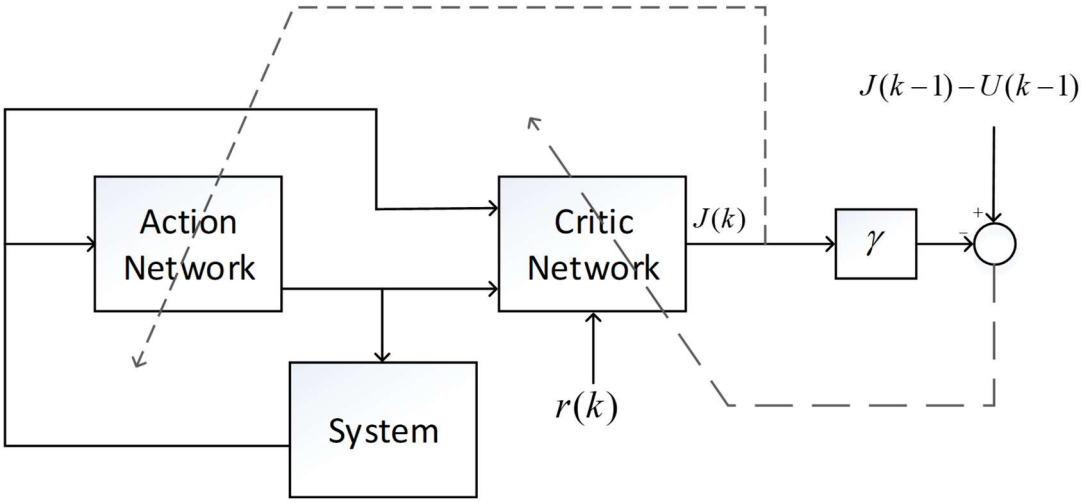

Figure 4. The block diagram of HDP including two subnetworks

3.1. CRITIC NEURAL NETWORK

The Bellman's equation or the cost-to-go function can be written as

$$J(k) = \sum_{k=0}^{\infty} \gamma^i U(k+1). \tag{10}$$

A discount factor is presented by γ, in the range of zero and one, to highlight the significance of the future costs, and to guarantee that the cost-to-go function is constrained in the infinite horizon. Function $U(k)$ is the utility function that, in this paper, is defined as:

$$U(k) = \sqrt{K_P e_P^2 + K_Q e_Q^2 + K_f e_f^2} \tag{11}$$

where e_f , e_Q, and e_P, are the error signals for the inverter frequency, reactive power, and active power, respectively defined as:

$$e_f = f_g - f \tag{12}$$

$$e_Q = Q_{set} - Q \tag{13}$$

$$e_P = P_{set} - P \tag{14}$$

and K_f, K_P, K_Q are the frequency coefficient, the reactive power coefficient, and the active power coefficient, respectively. A feedforward fully-connected multilayer neural network is used to perform as the critic network, which is depicted in Figure 5. The proposed network includes two hidden layers and eight nodes at each layer. The proposed critic network in this paper, is based on state-value-functions. It means that the cost-to-go function can be defined based on the system state variables. The main state variables of the system are the active/reactive error signals, the frequency deviation, and the power angle. The changes in reference signals alter the active/reactive error signals; therefor the active/reactive power are also required to be presented as state variables. Therefore, the state variable vector, which is the input to the critic network, can be defines as follows.

$$IN_{\{critic\ network\}} = \left[P\ Q\ e_p\ e_q\ e_f\ \theta_i\ E\right]. \tag{15}$$

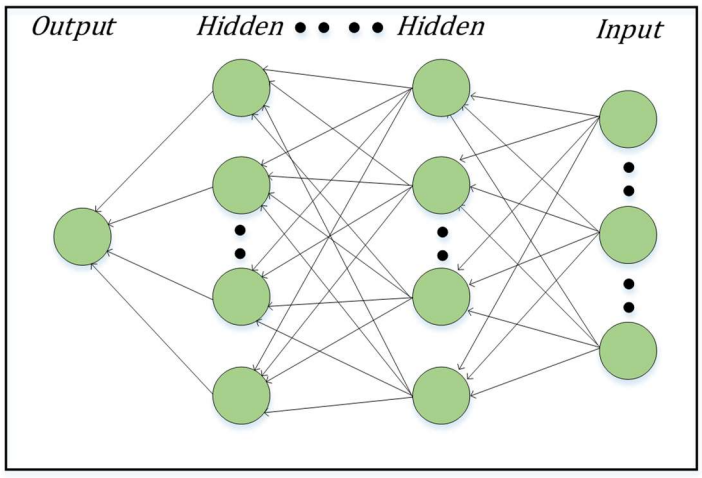

Figure 5. Fully connected feedforward neural network

The critic network is trained forward in time, because the system operates in real-time. The goal of the critic network is to estimate $J(\cdot)$; therefore, by subtracting two successive cost-o-go function using the Bellman's equation, the error signal can be written as:

$$\sum_{k}[J(k) - \gamma J(k+1) - U(k)]^2. \tag{16}$$

The weights are updated using the gradient decent method as

$$W_{critic}(k+1) = W_{critic}(k) + \Delta W_{critic} \tag{17}$$

where W_{critic} is the critic network's weight and α_c is the learning rate.

3.2. ACTION NEURAL NETWORK

The main objective of the action network is to generate the control signal to minimize the J function for the immediate future. The action network is formed similar to the critic network as a feedforward neural network with two hidden layers and four nodes at each layer. The input signal to the action network is a vector similar to the input of the critic network; however, it does not include the voltage magnitude and can be written as

$$IN_{\{action\ network\}} = \left[P\ Q\ e_p\ e_q\ e_f\ \theta_i\right]. \tag{18}$$

The output of the action network is the peak value of the output voltage of the inverter $(E(k))$. This peak value can be selected in a range of the minimum and the maximum of the acceptable voltage. The maximum voltage is also bounded by the voltage of the DC link where $V_{max} \approx 0.62\ V_{dc}$ [28].

The backpropagation procedure is utilized to update weights in the action network. The objective is to minimize the cost-to-go function. Therefore, the derivative of the cost-to-

go function with respect to the control signal is used as the training feedback signal for the action network.

$$\zeta = \sum_{k} \frac{\partial J(k+1)}{\partial E(k)} \tag{19}$$

This signal can be used to update the weights as

$$\Delta W_{action} = -\alpha_a \zeta \frac{\partial \zeta}{\partial W_{action}} \tag{20}$$

$$W_{action}(k+1) = W_{action}(k) + \Delta W_{action} \tag{21}$$

where α_a and W_{action} are the learning rate and the action network weights, respectively. Hyper parameters selection, and training procedure are two of the most important concerns when it comes to the neurocontrol techniques. In order to fine tune the hyper parameters, such as learning rate or the discount factor, the trial-and-error technique is used to achieve the best performance. Another main issue which is required to be discussed is whether the data for the training procedure is enough or not. Since the controller never stops learning, to stay updated for any changes in the system, there is no reason to be concerned about the size of the training set. In cases that model dependent HDP (MDHDP) is implemented, a neural network is utilized which models the dynamic behavior of the system. Pretraining this neural network improves the performance of the controller. Considering that the model of a grid-connected VSG has small number of inputs and outputs, a data set with couple of thousand samples are enough to pretrain the system. These samples can be collected in the order of seconds. However, in this paper an action dependent (ADHDP) is utilized [29].

4. SIMULATION RESULTS

The proposed HDP-based, grid-connected VSG is illustrated in Figure 6. As depicted, the proposed approach is formed by replacing the conventional I/PI controller in the traditional VSG with an HDP controller. In this figure, the "network input generator" is implemented to prepare the input vector for the neural networks.

The training procedure is listed as follows:

1. Generate a random initial state.
2. Generate a random set of active/reactive power references.
3. Initialize the weights of the networks randomly.
4. Keep updating the Weights.

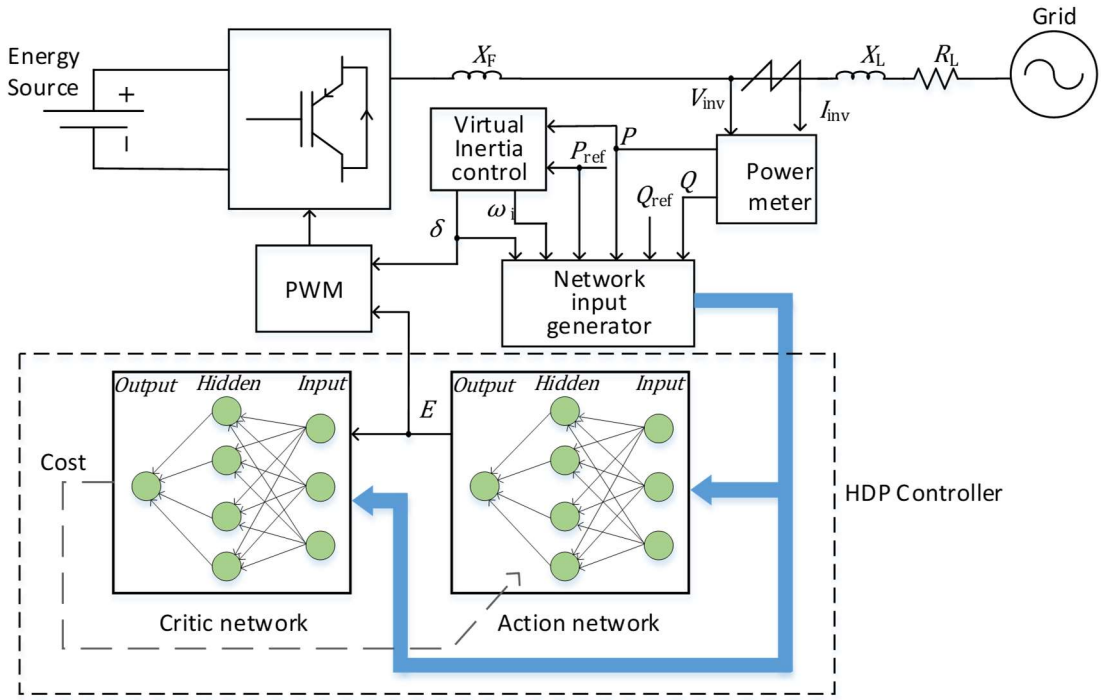

Figure 6. The grid-connected VSG controlled by a neural-network-based HDP

Table 1. PI parameters

Parameter	Value
Inductive grid	
K_p	0.8
K_i	65
Resistive grid	
K_p	0.4
K_i	30

Table 2. VSG and power system parameters

Parameter	Value	Unit
DC voltage	250	V
AC line voltage	110	V
AC frequency	60	Hz
Moment of inertia	1	$Kg.m^2$
Frequency droop	%2	--
Inverter power rating	5	kW
Inductive line		
Filter inductance	1	μH
Line inductance	100	μH
Line resistance	10	mΩ
Resistive line		
Filter inductance	1	μH
Line inductance	1	μH
Line resistance	500	mΩ
HDP parameters		
γ	1	
Sampling time	1	ms
$[\alpha_c \ \alpha_c]$	[1 1]	--
$[k_P \ \ k_Q \ \ k_f]$	[1 1 0]	--

Table 2 illustrates the system parameters, and the controller parameter for the conventional VSG are provided in Table 1.

.

4.1. INDUCTIVE GRID

The performance of a conventional VSG and an HDP-based VSG is illustrated in Figure 7. In this figure, the inverter is connected to an inductive grid. As discussed in Section 2, the decoupled control assumption in the inductive grid is valid; therefore, the performance of the conventional VSG is acceptable. In this part, different active and reactive power references are applied to both the conventional and HDP-based VSG. A precise look into the magnified version confirms that the proposed controller performs slightly faster with a smaller percentage of overshoot. The reason is that the conventional controllers are designed for the nominal operating point, and changes in the operating point affect the performance. In addition, the system is not purely inductive; hence, the

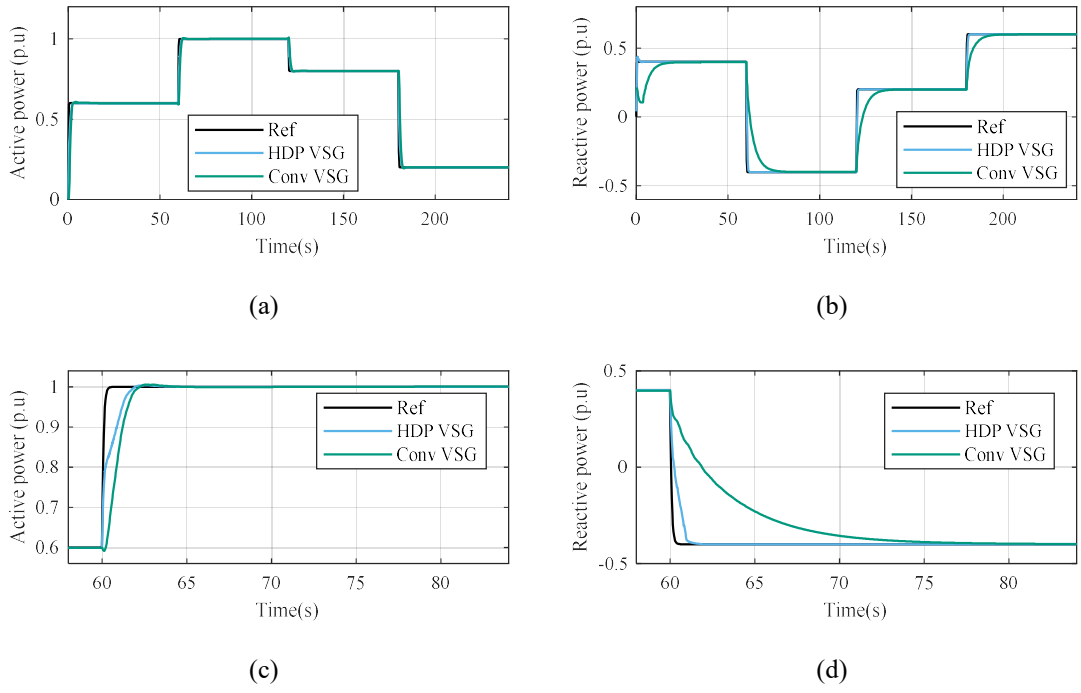

Figure 7. The active/reactive tracking of a conventional VSG and an HDP-based VSG in an inductive grid connection

proposed HDP-based VSG performs better by applying the impact of both the inverter voltage and power angle in controlling the reactive power.

4.2. RESISTIVE GRID

In this part, the inverter is connected to a resistive grid. The performance of the conventional and HDP-based VSG is depicted in Figure 8. As discussed in Section 2, in noninductive grids, the performance of the conventional VSG is not acceptable. As it was expected from the mathematical point of view, the conventional VSG generates active/reactive power fluctuations. On the other hand, the HDP-based VSG shows a better performance in tracking the active and reactive power references. The reason is that the system adjust itself with any power angles. In other word, the action neural

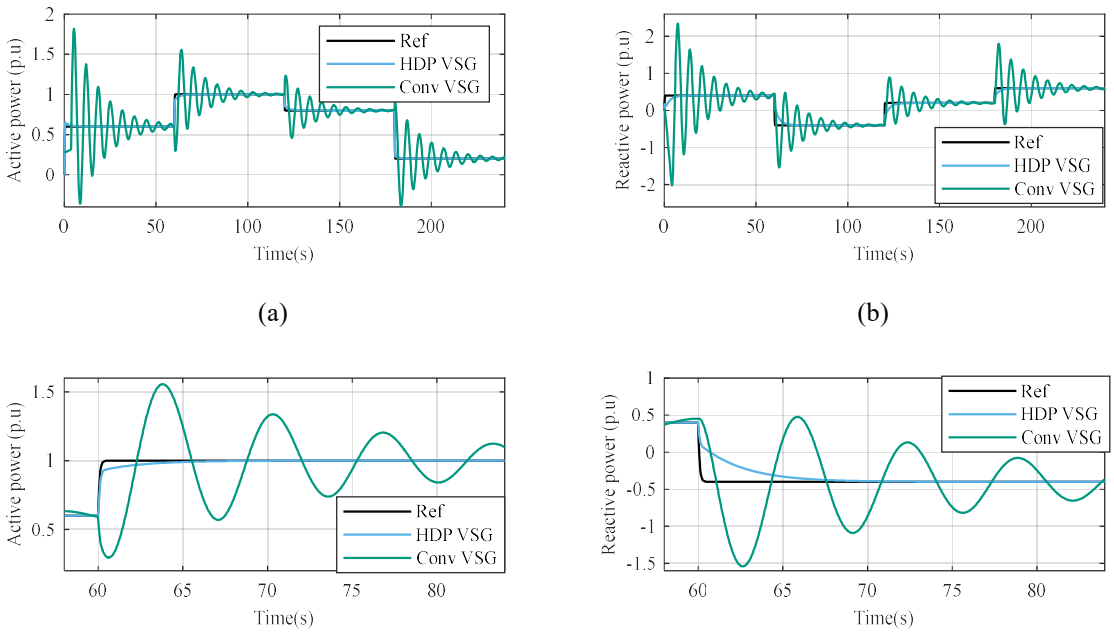

Figure 8. The active/reactive tracking of a conventional VSG and an HDP-based VSG in a resistive grid connection

network adjust itself to control the inverter voltage to regulate both the active and the reactive power.

5. EXPERIMENTAL RESULTS

A laboratory prototype is prepared to evaluate the performance of the proposed technique. A grid-connected inverter with the power rating of 1 kVA with the grid connection compatibility is set up. The grid voltage is a three-phase with a 190V/60Hz line-line voltage. The control algorithm is implemented in a Texas Instruments signal processor TMS320F28377, and MATLAB R2018a. The direct current control, the traditional VSG, and the HDP-based VSG are implemented to regulate the active and reactive power and the frequency. The prototype is shown in Figure 9. As shown, the prototype includes a DC voltage source that provides the inertia needed for the DC side.

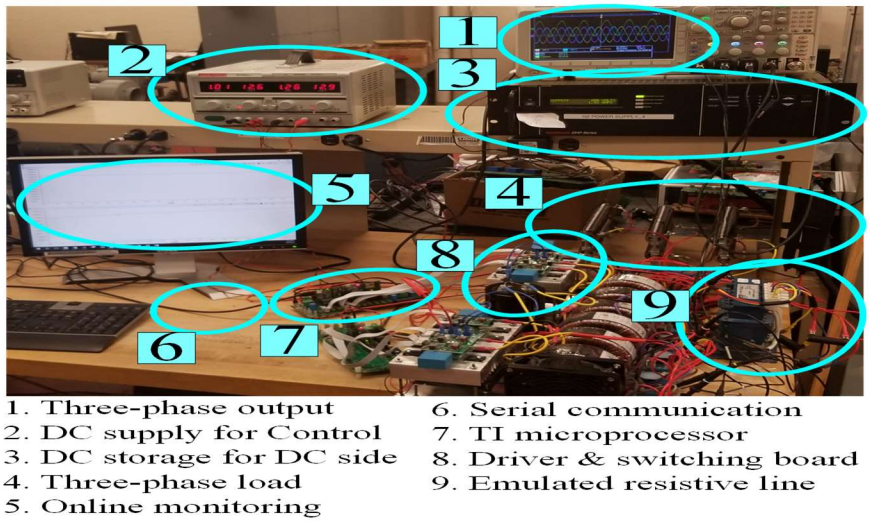

Figure 9. Three-phase grid-connected inverter test bed

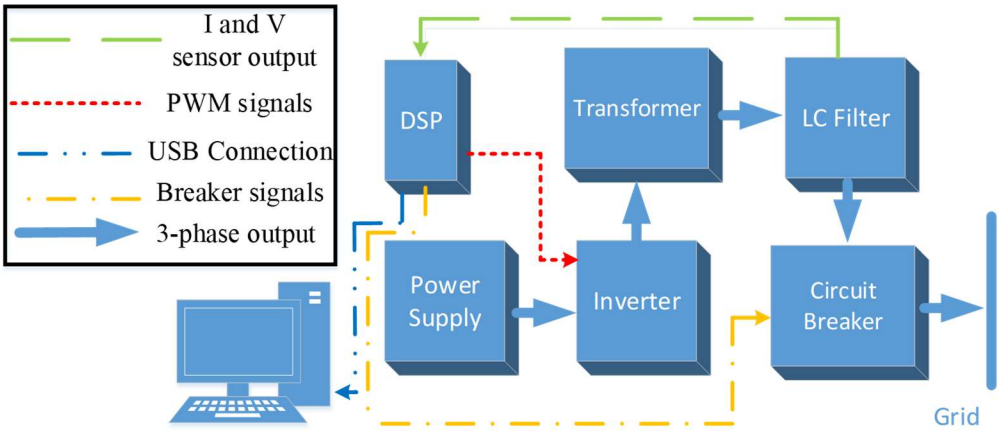

Figure 10. The block diagram of the test bed

A three-phase inverter is connected to the grid via a three-phase transformer to boost up the voltage and to provide the isolation. Three relays protect the system from faults. The embedded analog-to-digital converter can read the inverter current and voltage. A USB to serial adaptor provides the connection mechanism between the microcontroller and the computer. Data acquisition and basic protections such as voltage and current are implemented inside the microcontroller. The computationally expensive calculations, such as the neural network training, are implemented in the computer. At each control cycle, the weights are updated to provide the ability to adaptively control the system. Figure 10 illustrates the block diagram of the experimental control mechanism.

5.1. GRID CONNECTING PROCEDURE

The goal of this paper is to control the power interaction between the grid and the inverter by regulating the frequency and the voltage of the inverter. One of the most critical points of controlling a grid-connected inverter is to connect it to the grid. There are several techniques to connect an inverter into the grid, and this paper implemented

two of them. The first method uses a PLL to find the frequency and the theta of the grid in order to connect the inverter to the grid in the synchronized mode. However, it was discussed that in the transient conditions, the performance of the PLL is highly affected. A low-pass filter can be used to decrease the imperfect performance during the transient time; however, it is not the best solution. Therefore, the second method, zero crossing, is implemented to connect the inverter into the grid. In this technique, by reading the voltage, the inverter is connected to the grid when the grid voltage crosses the zero voltage. This method is easier to implement and does not have the disadvantages of PLL-based techniques. The only drawback of this technique compared to the PLL-based techniques is that the inverter can only be connected to the grid when the voltage crosses zero, which is not the concern of this paper.

5.2. PROTECTION

The experimental testbed is designed for a specific operating point. Therefore, to protect the electrical elements, a protection system is required. In this paper, the protection system includes two mechanisms. The first mechanism protects the electrical elements from a fault current in a short period of time. In order to do that, the switch currents are read at every control cycle. If the current is higher than the fault threshold, it will trigger the relays and disconnects the inverter. The second mechanism is implemented to protect the inverter from injecting excessive power to the grid. In virtual inertia techniques, a mechanism is needed to limit the power injected to the grid. In order to implement the second mechanism, using the virtual rotating angle, the switch currents in the three-phase platform will be transformed into a d-q platform. If the current is

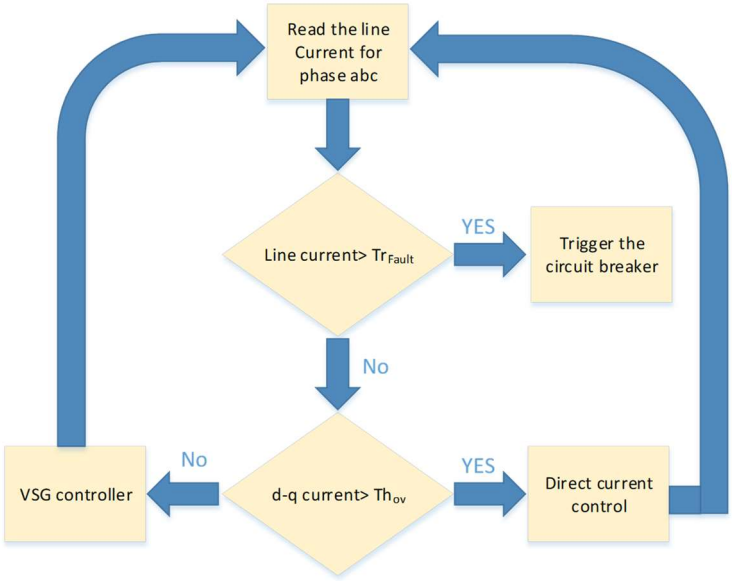

Figure 11. The block diagram of the protection

greater than the overload threshold, the control mechanism moves back to the conventional direct-current mode. Figure 11 shows the block diagram of the proposed protection mechanism.

5.3. TRAINING THE NETWORKS

Similar to all of the adaptive critic design techniques, the heuristic dynamic programming includes two main networks. Therefore, the training procedure is divided into two different mechanisms. In order to train the action network, the critic network is required to provide the feedback signal. This signal evaluates the performance of the action network. As mathematically explained in Section 3, the action network's weights are updated. The highlighted concern in training the action network is the accuracy of the feedback signal. Regarding the timing of the training procedure of the HDP network, there are two different approaches. In the first approach, the action network and the critic

network are trained simultaneously, which means that until the critic network is trained, the feedback signal to train the action network is not accurate. However, when the critic network is well-trained, the feedback can be used to train the action network and to update its weights. Considering the fact that training the critic network is time consuming, the action network performance is not improved. Controlling a grid-connected inverter with a random controller for a period leads the system to instability. Although the first approach can be applied to several applications, it is not applicable for controlling a grid-connected inverter. In the second approach, the critic network is pretrained in advance; afterwards, the online training procedure keeps the critic network tuned. To train the critic network, a stable conventional PI-based VSG scheme regulates the voltage and the frequency of the inverter. This procedure starts with a random state and uses the feedback signal at the next step. By using Bellman's equation as the feedback signal and implementing (5) and (6), the critic network is trained and the network weights are updated. The critic network output is the cost-to-go value. The error signal can be generated by subtracting the estimated cost-to-go value and the discounted, estimated cost-to-go value for the next step and comparing it with the utility function. This error signal can be used to train the critic network. Based on the amount of time needed to train the network, a time step of 1 millisecond is selected. By reading the state variables through the DSP and computing the active/reactive power, utility function, frequency, and error signal, the data package is ready to be sent to the computer. The training procedure and updating-weights process is utilized by the computer. This procedure continues until the critic network is trained. To train the critic network, 500

random initial states were generated and 50000 data sets were collected. Using the backpropagation technique, the gradient decent is used to train the network.

After training the critic network, the conventional PI-based VSG will be replaced by the HDP-based VSG. Similar to the critic network training procedure, the time step to train the action network is 1 millisecond. The action network is trained by applying random active and reactive power references, receiving the feedback signal from the critic network, and transmitting all of the data to the computer. Equations (7) and (8) are used to train the action network. After finishing the training procedure, the proposed VSG approach can operate in nominal conditions. The training procedure continues for the whole operating time to adjust and fine-tune the network parameters.

As mentioned, the conventional VSGs are designed based on linearized model of the system. Consequently, changes in system's parameters or operating point affects the behavior of the controller. Therefore, the parameters are required to be tuned or even redesigned. On the other hand, the neural network characteristics of the proposed technique adaptively tunes itself in various conditions. The computational complexity is the main concern of the proposed method, specially in experimental implementation. All the neural networks are required to be perform and trained in a control cycle, which is defined by the switching frequency. Implementation of feedforward neural networks, gradient decent backpropagation, and nonlinear activation functions are computationally expensive. There are two main approaches to tackle this concern. In the first approach the controller is implemented in the microcontroller with less computational power. The controller is required to be simplified to meet the timing constraints. Decreasing neurons or using look-up tables to perform as the activation functions are some of the solutions.

However, this approach decreases the accuracy of the system. In the second approach, controller structure is implemented into a computer. In this approach the microcontroller collects the system data and transfer them into the computer. The computer computes the control signal and trains the neural networks and send the control command into the microcontroller. Finally, the microcontroller uses the control command to generates the switching signals.

It was explained in Section 2 that the conventional VSGs are suitable for inductive grids; however, their performance is significantly affected when facing a noninductive/resistive grid. The simulation results in Section 4 also confirm this. Therefore, to evaluate the performance of the proposed VSG, only the resistive grid is

Table 3. PI parameter for the experimental testbed

Parameter	Value
Resistive grid	
K_p	0.19
K_i	40

Table 4. Experimental testbed parameters

Parameter	**Value**	**Unit**
VSG		
DC voltage	400	V
AC line voltage	110	V
AC frequency	60	Hz
Moment of inertia	0.5	Kg. m2
Frequency droop	%4	--
Inverter power rating	1	kW
Line Parameters		
Filter reactance	900	mΩ
Line reactance	150	mΩ
Line resistance	1800	mΩ

studied illustrates the parameters of the test bed and the PI parameter used to control the conventional VSG is presented in Table 3 and Table 4.

5.4. RESISTIVE GRID CONNECTION

The experimental results regarding the changes in active power reference is illustrated in Figure 13. In this figure, the green (top) waveform presents the active power and the blue (bottom) waveform presents the reactive power. For the first part of the experiment, the active power reference changes in {0.1, 0.5, 0.25, 0.6, 0.15, 0.1} (p.u), while the reactive power reference is fixed at 0.1 p.u. An analog signal is used to illustrate the active and a reactive power on the oscilloscope. The signal presenting the active power is tuned in a way that maps the power -1000 to 1000 W into an analog voltage in ranging from zero to five volts. The signal presenting the reactive power is tuned in a way that maps the reactive power in [-700, 700] (VAR) to an analog voltage in [0, 5] (V). In this figure, the conventional VSG performance facing changes in the active power is shown in (a), and the magnified view is shown in (b). To compare the results with the proposed HDP-based VSG controller, (c) illustrates the performance of the HDP-based VSG facing the same changes in active power. The magnified version is illustrated in (d). As expected from the mathematical modeling proposed in Section 2 and the simulation results in Section 4, the conventional VSG control scheme is unable to perform well when it is connected to a resistive grid. The ringing and oscillation in active and reactive power illustrates the weakness of the conventional PI-based VSGs. On the other hand, the HDP-based VSG control scheme adapts its input regarding the grid parameters. As the experimental results show, the HDP-based VSG performs better in

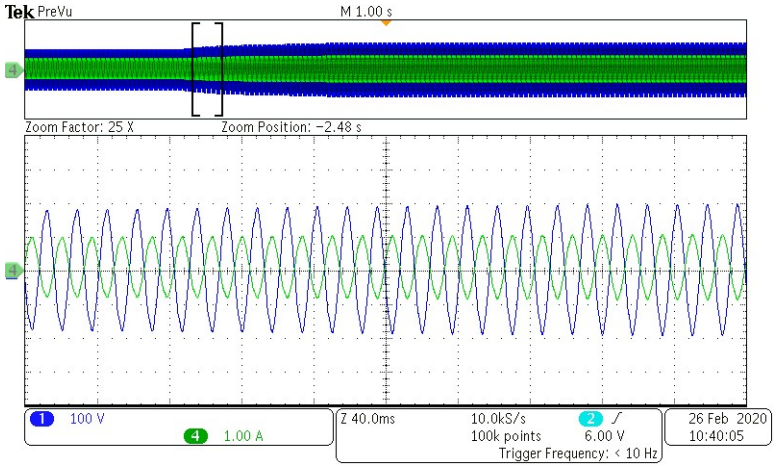

Figure 12. The phase output voltage and the line current of synchronverter after the low-pass filter

tracking the power references. The frequency and voltage performance of the proposed HDP-based VSG is depicted in Figure 12. As shown, the proposed controller tracks the references for the active and reactive power smoothly by changing the voltage and the phase of the inverter. In this figure, the green wave shows the line current, and the blue waveform depicts the inverter output voltage.

In the second step, we perform the experiment under the conditions that the active power reference is fixed and the reference of the reactive power changes. The scaling condition used to illustrate the active and the reactive power on the oscilloscope, is similar to the first part of the experiment. In this part, the reference of the active power is fixed on 0.1 p.u and the reactive power changes in {0.1, -0.15, -0.3, 0.4, 0.15, 0.1} (p.u). To illustrate the effectiveness of the proposed control scheme, the performance of the conventional PI-based VSG, and the performance of the proposed HDP-based VSG are shown in Figure 12. In this figure, the performance of the conventional VSG is shown in (a). The magnified view is illustrated in (b), the performance of the HDP-based VSG is

shown in (c), and the magnified waveform is illustrated in (d). Needless to say, the experimental results highlighted the weakness of the conventional VSGs. As mentioned, a stable PI-based VSG can lead to instability if the operating point is different from what the system is designed for. It is shown, for some operating points, the traditional VSG is unstable and cannot regulate the power. The HDP-based VSG tracks the references with much less oscillation and with lower overshoots. The HDP characteristics of the controller guarantee optimal performance in regulating the voltage and the frequency while tracking the active and the reactive references.

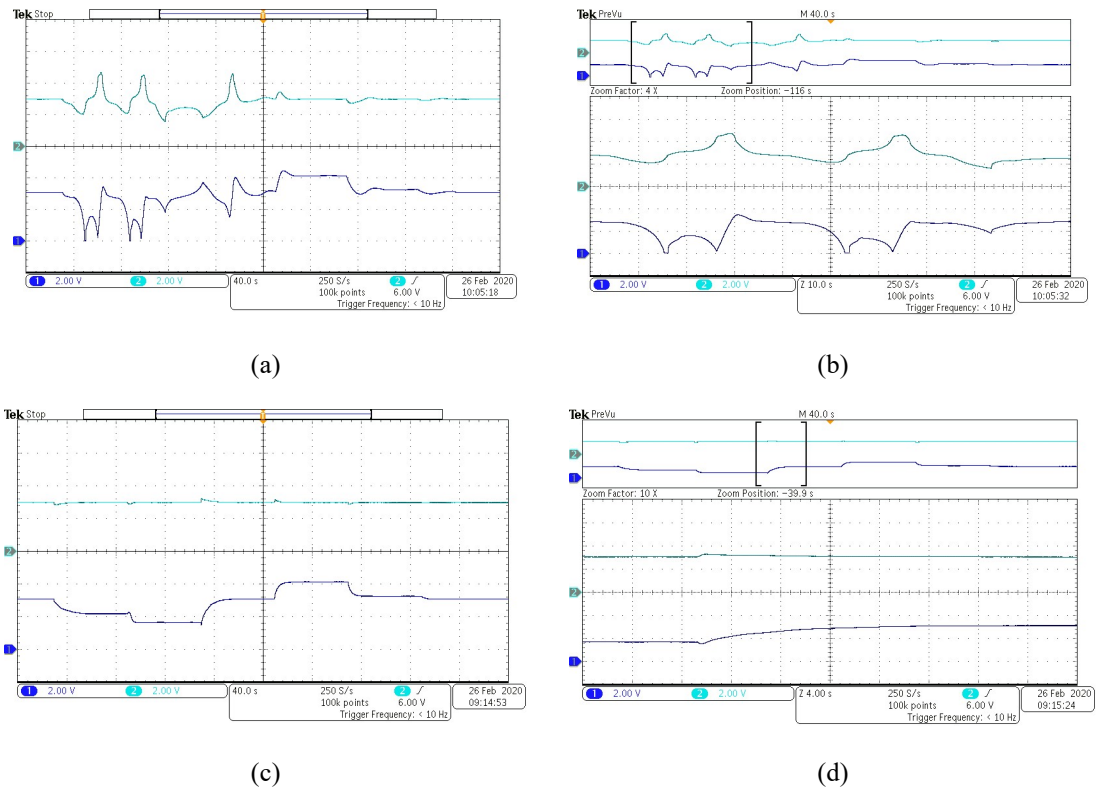

Figure 13. Injected active and reactive power from a three-phase grid connected synchronverter facing reactive power reference changes (a) traditional VSG, (b) magnified response for traditional VSG, (c) HDP-based VSG (d) magnified waveform of HDP-Value VSG

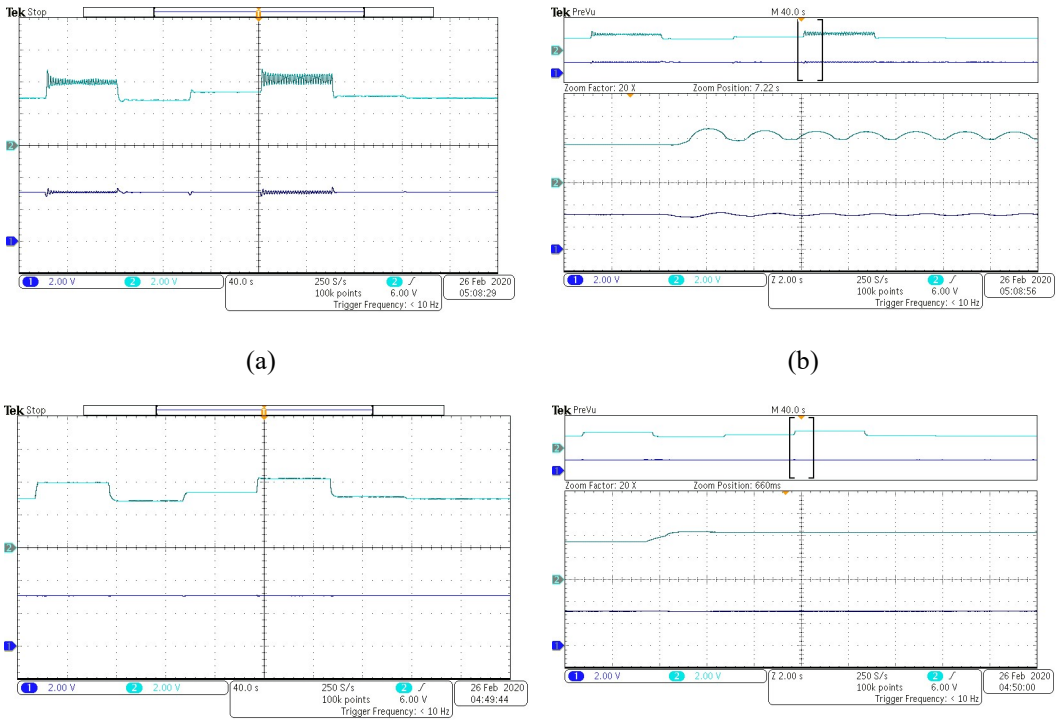

Figure 14. Injected active and reactive power from a three-phase grid connected synchronverter facing active power reference changes (a) traditional VSG, (b) magnified response for traditional VSG, (c) HDP-based VSG (d) magnified output waveform of HDP-based VSG

6. CONCLUSION

By increasing the penetration of the renewable energy sources into the power grid, the utilization of the three-phase grid-connected inverters has increased. The most common technique to control grid-connected inverters is the direct current/power control, which decreases the system inertia. This significantly affects the stability of the power system in weak grids. The virtual-inertia-based technique has been introduced to overcome those drawbacks, but the PI-based design and decoupled assumption features of the conventional VSGs affects the performance of the controller when the system faces noninductive grids or various operating points. An HDP-based technique, as a machine-

learning algorithm, is proposed in this paper to tackle the aforementioned drawbacks and to enable the inverter to optimally regulate the voltage and the frequency. The simulation results and the experimental results are shown to evaluate the performance of the proposed HDP-based controller in facing critical conditions. The performance of the proposed approach is compared with the performance of the conventional VSG controllers. As illustrated, an adaptive-critic-based controller with a well-tuned neural network can improve the performance of the virtual inertia-based grid-connected inverters.

REFERENCES

[1] Blaabjerg F, Teodorescu R, Liserre M, Timbus A V. Overview of control and grid synchronization for distributed power generation systems. IEEE Trans Ind Electron 2006;53:1398–409. https://doi.org/10.1109/TIE.2006.881997.

[2] Zhong QC. Power-Electronics-Enabled Autonomous Power Systems: Architecture and Technical Routes. IEEE Trans Ind Electron 2017;64:5907–18. https://doi.org/10.1109/TIE.2017.2677339.

[3] Panamtash H, Zhou Q, Hong T, Qu Z, Davis KO. A copula-based Bayesian method for probabilistic solar power forecasting. Sol Energy 2020;196:336–45. https://doi.org/10.1016/j.solener.2019.11.079.

[4] Bevrani H, Ise T, Miura Y. Virtual synchronous generators: A survey and new perspectives. Int J Electr Power Energy Syst 2014;54:244–54. https://doi.org/10.1016/j.ijepes.2013.07.009.

[5] Silva B, Moreira CL, Seca L, Phulpin Y, Lopes JAP. Provision of inertial and primary frequency control services using offshore multiterminal HVDC networks. IEEE Trans Sustain Energy 2012;3:800–8. https://doi.org/10.1109/TSTE.2012.2199774.

[6] Asrari A, Mustafa M, Ansari M, Khazaei J. Impedance Analysis of Virtual Synchronous Generator-Based Vector Controlled Converters for Weak AC Grid Integration. IEEE Trans Sustain Energy 2019;10:1481–90. https://doi.org/10.1109/TSTE.2019.2892670.

[7] Miao Z, Fan L, Osborn D, Yuvarajan S. Wind farms with HVdc delivery in inertial response and primary frequency control. IEEE Trans Energy Convers 2010;25:1171–8. https://doi.org/10.1109/TEC.2010.2060202.

[8] Zhong QC, Weiss G. Synchronverters: Inverters that mimic synchronous generators. IEEE Trans Ind Electron 2011;58:1259–67. https://doi.org/10.1109/TIE.2010.2048839.

[9] Beck HP, Hesse R. Virtual synchronous machine. 2007 9th Int. Conf. Electr. Power Qual. Util. EPQU, 2007. https://doi.org/10.1109/EPQU.2007.4424220.

[10] Driesen J, Visscher K. Virtual synchronous generators. IEEE Power Energy Soc. 2008 Gen. Meet. Convers. Deliv. Electr. Energy 21st Century, PES, 2008. https://doi.org/10.1109/PES.2008.4596800.

[11] Meng X, Liu J, Liu Z. A Generalized Droop Control for Grid-Supporting Inverter Based on Comparison between Traditional Droop Control and Virtual Synchronous Generator Control. IEEE Trans Power Electron 2019;34:5416–38. https://doi.org/10.1109/TPEL.2018.2868722.

[12] Chen J, O'Donnell T. Parameter constraints for virtual synchronous generator considering stability. IEEE Trans Power Syst 2019;34:2479–81. https://doi.org/10.1109/TPWRS.2019.2896853.

[13] Du W, Fu Q, Wang HF. Power System Small-Signal Angular Stability Affected by Virtual Synchronous Generators. IEEE Trans Power Syst 2019;34:3209–19. https://doi.org/10.1109/TPWRS.2019.2896149.

[14] Karimi A, Khayat Y, Naderi M, Dragičević T, Mirzaei R, Blaabjerg F, et al. Inertia Response Improvement in AC Microgrids: A Fuzzy-Based Virtual Synchronous Generator Control. IEEE Trans Power Electron 2020;35:4321–31. https://doi.org/10.1109/TPEL.2019.2937397.

[15] Fathi A, Shafiee Q, Bevrani H. Robust frequency control of microgrids using an extended virtual synchronous generator. IEEE Trans Power Syst 2018;33:6289–97. https://doi.org/10.1109/TPWRS.2018.2850880.

[16] Shi K, Ye H, Song W, Zhou G. Virtual Inertia Control Strategy in Microgrid Based on Virtual Synchronous Generator Technology. IEEE Access 2018;6:27949–57. https://doi.org/10.1109/ACCESS.2018.2839737.

[17] Choopani M, Hosseinian SH, Vahidi B. New Transient Stability and LVRT Improvement of Multi-VSG Grids Using the Frequency of the Center of Inertia. IEEE Trans Power Syst 2020;35:527–38. https://doi.org/10.1109/TPWRS.2019.2928319.

[18] Li J, Wen B, Wang H. Adaptive virtual inertia control strategy of VSG for micro-grid based on improved bang-bang control strategy. IEEE Access 2019;7:39509–14. https://doi.org/10.1109/ACCESS.2019.2904943.

[19] Saadatmand S, Nia MSS, Shamsi P, Ferdowsi M, Wunsch DC. Neural Network Predictive Controller for Grid-Connected Virtual Synchronous Generator. 2019 North Am. Power Symp., IEEE; 2019, p. 1–6. https://doi.org/10.1109/NAPS46351.2019.9000386.

[20] Shi R, Zhang X, Hu C, Xu H, Gu J, Cao W. Self-tuning virtual synchronous generator control for improving frequency stability in autonomous photovoltaic-diesel microgrids. J Mod Power Syst Clean Energy 2018;6:482–94. https://doi.org/10.1007/s40565-017-0347-3.

[21] Wang F, Zhang L, Feng X, Guo H. An Adaptive Control Strategy for Virtual Synchronous Generator. IEEE Trans Ind Appl 2018;54:5124–33. https://doi.org/10.1109/TIA.2018.2859384.

[22] Yang H, Xie X, Kadoch M. Intelligent resource management based on reinforcement learning for ultra-reliable and low-latency IoV communication networks. IEEE Trans Veh Technol 2019;68:4157–69. https://doi.org/10.1109/TVT.2018.2890686.

[23] Yang H, Alphones A, Zhong W De, Chen C, Xie X. Learning-Based Energy-Efficient Resource Management by Heterogeneous RF/VLC for Ultra-Reliable Low-Latency Industrial IoT Networks. IEEE Trans Ind Informatics 2020;16:5565–76. https://doi.org/10.1109/TII.2019.2933867.

[24] Saadatmand S, Nia MSS, Shamsi P, Ferdowsi M, Wunsch DC. Heuristic Dynamic Programming for Adaptive Virtual Synchronous Generators. 2019 North Am. Power Symp., IEEE; 2019, p. 1–6. https://doi.org/10.1109/NAPS46351.2019.9000393.

[25] Saadatmand S, Nia MSS, Shamsi P, Ferdowsi M. Dual Heuristic Dynamic Programing Control of Grid-Connected Synchronverters. 2019 North Am. Power Symp., IEEE; 2019, p. 1–1. https://doi.org/10.1109/NAPS46351.2019.9000382.

[26] Ashabani M, Mohamed YARI. Novel comprehensive control framework for incorporating VSCs to smart power grids using bidirectional synchronous-VSC. IEEE Trans Power Syst 2014;29:943–57. https://doi.org/10.1109/TPWRS.2013.2287291.

[27] Bellman R, Dreyfus S. Functional Approximations and Dynamic Programming. Math Tables Other Aids to Comput 1959;13:247. https://doi.org/10.2307/2002797.

[28] Choi W, Wu Y, Han D, Gorman J, Palavicino PC, Lee W, et al. Reviews on grid-connected inverter, utility-scaled battery energy storage system, and vehicle-to-grid application - Challenges and opportunities. 2017 IEEE Transp. Electrif. Conf. Expo, ITEC 2017, Institute of Electrical and Electronics Engineers Inc.; 2017, p. 203–10. https://doi.org/10.1109/ITEC.2017.7993272.

[29] Prokhorov D V., Wunsch DC. Adaptive critic designs. IEEE Trans Neural Networks 1997;8:997–1007. https://doi.org/10.1109/72.623201.

III. THE ACTIVE AND REACTIVE POWER REGULATION OF GRID-CONNECTED VIRTUAL INERTIA-BASED INVERTERS BASED ON THE VALUE GRADIENT LEARNING

Sepehr Saadatmand, Pourya Shamsi, and Mehdi Ferdowsi

Department of Electrical Engineering, Missouri University of Science and Technology, Rolla, MO 65409

ABSTRACT

The value gradient learning (VGL) is one of the most powerful state-of-the-art methods in the field of machine learning. In this paper, a dual heuristic dynamic programming (DHP) control technique, as the most straightforward VGL, is introduced to control a virtual inertia-based grid-connected inverter. The stability of power systems is extremely affected by the increase in the penetration of fast-responding inertia-less inverters. The virtual synchronous generator (VSG) control scheme addresses this drawback; however, the proposed technique is not designed for noninductive grids, and it is sensitive to the operating point due to its linear control-based inherence. The DHP approach as an adaptive critic design with three embedded neural networks is presented in this paper to overcome the aforementioned drawbacks. On the contrary of the conventional PI-based synchronverters that operate based on two decoupled single-input single-output (SISO), the proposed method provides a multiple-input multiple-output (MIMO) platform to regulate the power and frequency of a grid-connected synchronverter. The simulation and experimental results are provided to evaluate the effectiveness of the proposed DHP-based VSG. The results illustrate that a well-designed

well-trained DHP-based VSG demonstrates an optimal performance in different scenarios compared to the conventional PI-based VSG.

Keywords: Adaptive critic design, DC/AC converters, Dual heuristic dynamic programming, Machine learning, Reinforcement learning, Value gradient learning, Virtual inertia, Synchronverter

1. INTRODUCTION

Recently, the energy and environmental crises have become two of the most critical concerns for all governments worldwide. Consequently, the implementation of distributed energy (DG) sources has rapidly increased [1], [2]. Renewable energy sources (RESs), such as wind farms and solar panels, have attracted significant attention due to their sustainability and environmentally friendly behavior. The traditional power grid has been significantly affected by the increase in penetration of RESs [3]. The existing kinetic inertia in the enormous rotating parts of synchronous generators plays a vital role in stabilizing power systems. The frequency stability is directly related to the balance between the demand and generation. This kinetic inertia enables the power system to release/store energy during transients, which improves the performance of the grid by maintaining the balance between the demand and generation. The most common technique to connect RESs into the power grid is via three-phase direct current/power inverters. The fast-responding inertia-less inherences of these converters considerably reduces the power system stability and robustness, especially in weak grids, such as micro grids [4]–[6].

Direct current/power grid-connected inverters require the frequency and the phase angle of the grid to use it as a reference. In order to read these essential data, the phase-locked-loop (PLL) is used. The behavior of PLLs is highly nonlinear, which affects their performance, especially during transients [7]. Therefore, to address drawbacks regarding the inertia and PLL, the concept of the virtual synchronous generator (VSG) has been introduced. The concept of VSG is a control scheme to govern three-phase inverters, which emulates the mechanical behavior of a synchronous generator (SG) [8]–[10]. The mechanical behavior of synchronous generators, known as the swing equation, functions as the main part of the VSG concept. Several studies have implemented the VSG control scheme to regulate the voltage and frequency of inverters based on the power balance equations and state of charge (SoC) of the storage device [11], [12], in which no DG is implemented. The concept of static synchronous generator (SSG) was introduced in [13] which performs like VSG but does not emulate the behavior of a synchronous generator exactly. Regarding the real synchronous generators, the power system stabilizer (PSS) damps the power oscillation; however, PSSs are unable to set the parameters in a highly nonlinear system in exitance of DGs. Since the VSG is only a control scheme it is not bounded by its mechanical characteristics and can be changed to perform better, for example by reducing the rate of change of frequency (RoCoF) [14].

Several studies have addressed new approaches regarding virtual-inertia-based techniques to control inverters. Ref [15] has proposed a stability analysis for a grid connected inverter when it performs as a VSG versus the droop control performance. In [16], it can be seen that considering the line and converter dynamics constraints the control parameters in a VSG design. The small-signal angular stability of a power

system is examined in [17] when it is connected to VSGs. A fuzzy control approach has been proposed in [18] to improve the stability of the power system and to decrease frequency fluctuations. To enhance the performance of VSGs, the characteristic of the alternating current has been studied in [19]. Ref [20] has proposed an extended synchronverter to improve the power system stability. By targeting the center of inertia frequency during short circuits, an enhanced method has been proposed for multi-VSG in [21].

The exact model of the system with accurate parameters is required for all the aforementioned techniques. However, a real power system includes uncertain conditions, approximated system model, missing or inaccurate system parameters. Several parameters of a power system can be read from the data sheet or can be measured which can be costly and time consuming. There are several nonlinear electric parts in a real power system such as transformers and inductors that can add to the nonlinearity and uncertainty of the model of the system. Besides, changing the power system parts, for example replacing a line or the aging concept, can alter the system parameters. The online autotuning characteristic of neural network-based machine learning techniques tackles these drawbacks.

In addition, the performance of a conventional VSG is not acceptable in noninductive grids, such as distributed systems. To tackle these concerns, several studies have addressed adaptive or machine learning-based approaches, such as the adaptive bang-bang technique [22] or the neural network predictive control [23]; however, the proposed methods lack online training. A neural network predictive VSG, self-tuning VSG in photovoltaic-diesel microgrids [24], and an adaptive VSG based on a small-

signal model [25] are also proposed. Nonetheless, these methods lack the implementation of an optimal, adaptive, and online-tuned VSG. To the best of the author's knowledge, only [26], [27] have all the aforementioned characteristics by implementing a neural-network-based adaptive critic design technique. A Value Learning (VL) technique is used in [26] to control the voltage of the inverter. The main drawback of the proposed technique is that the VL methods are significantly slow because it is required to search for the optimal solution in the whole state-space. To tackle this concern, a Value Gradient Learning technique is proposed in [27] to improve the training speed. There are two main draw backs regarding [27]: (i) it lacks the experimental implementation and (ii) the active/reactive combination is only used to control the voltage value, not the angle of the inverter. However, in this manuscript, both the active and reactive power errors are used regulate both the magnitude of the voltage and the frequency deviation of the inverter. The proposed techniques have not been evaluated by an experimental prototype.

The most highlighted contribution of this paper is to propose a dual heuristic programming as a value gradient learning technique to improve the power and frequency stability of grid-connected inverters. This paper does the following:

• Proposes a model-free neural network-based adaptive critic design technique to optimally regulate a grid connected VSG

• Presents online training to adjust the controller parameters when changes happen in the power system

• Presents a multiple-input and multiple-output (MIMO) to overcome the drawbacks of single-input and single-output (SISO) in traditional decoupled VSGs

The rest of the paper is organized as follows. Section 2 explains the concept of virtual synchronous generators and the weaknesses of the conventional VSG controller. The dual heuristic dynamic programing concept, design procedure, and training algorithm are discussed in Section 3. In section 4, the proposed DHP-based VSG is proposed, and the simulation results are provided to evaluate the effectiveness of the proposed technique. The implementation procedure including the system parameters are explained in Section 5, and the experimental results are provided.

2. GRID-CONNECTED VIRTUAL SYNCHRONOUS GENERATOR

As briefly mentioned in Section 1, the system model and parameters have direct impact on the effectiveness of the VSG control scheme. Transmission line parameters significantly alter the performance of conventional VSGs. In this section, the mathematical model of the virtual synchronous generator is explained. The impact of the transmission line parameters on the performance of VSG is illustrated by deriving the mathematical equation of the delivered power to the grid by the VSG.

2.1. VIRTUAL SYNCHRONOUS GENERATOR

The availability of an inertia source, which can keep the balance between the demand and the generation is one the most highlighted concerns in designing virtual-inertia-based inverters. To address this concern, it is assumed that a regular dc source is connected to the dc side. A block diagram of a virtual synchronous generator is depicted in Figure 1. The line resistance and reluctance are represented by R_L and X_L, and the

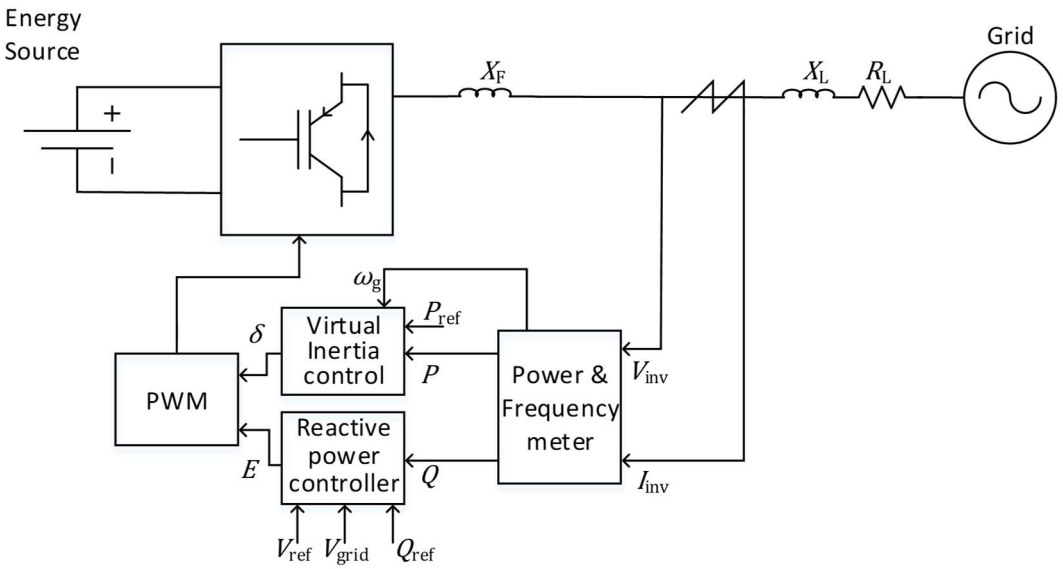

Figure 1. The block diagram of the traditional VSGs

equivalent inverter reluctance is represented by X_F. The so-called swing equation can be written as:

$$P_{in} - P_{out} = J\omega_i\left(\frac{d\omega_i}{dt}\right) + D\Delta\omega \tag{1}$$

where the input/reference power and the output power are P_{in} and P_{out}, the virtual moment of inertia and virtual droop coefficient are J and D, and the virtual rotating velocity is ω_i. The rotational frequency deviation can be defined as $\Delta\omega = \omega_i - \omega_g$, where ω_g represents the grid rotational frequency when the inverter is in grid-connected mode, or the reference rotational frequency when the inverter operates in stand-alone mode.

A grid-connected inverter is controlled by a pulse width modulation (PWM) unit. In order to generate the switching signals by the PWM unit, two parameters are required:

(i) the magnitude/peak of the voltage (E) and the phase of the voltage (δ) with respect to the grid phase as the reference phase, which can be computed as:

$$\delta = \int \Delta\omega \cdot dt. \tag{2}$$

The most common technique to control the voltage of a grid-connected inverter is to use conventional controllers, such as the integral (I) or the proportional-integral (PI), with the reactive power deviation as the error signal. In order to constraint the voltage, a voltage droop coefficient is also applied. Therefore, the inverter voltage can be computed as:

$$E = \frac{1}{K_i} \int \Delta Q \cdot dt - D_v \Delta V \tag{3}$$

where the integral coefficient, voltage droop coefficient, the reactive power deviation, and the voltage deviation are represented by K_i, D_v, $\Delta Q = Q_{ref} - Q_e$, and $\Delta V = V_{ref} - V_i$, respectively. The reference voltage, V_{ref}, is the grid voltage, and the reactive power reference is represented by Q_{ref}. The block diagram of the active-power-phase and reactive-power-voltage of a VSG are shown in Figure 2.

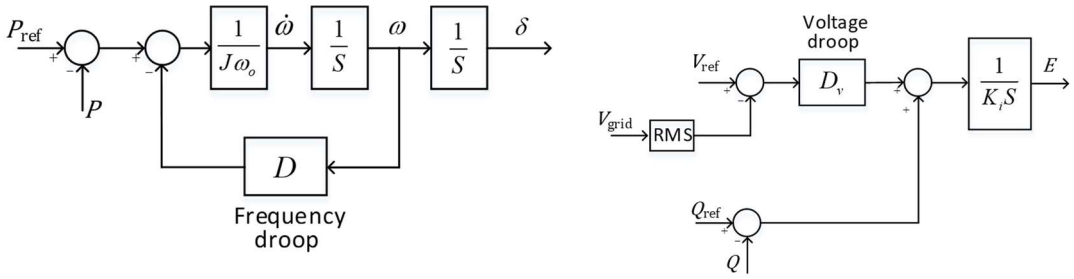

(a) (b)

Figure 2. The block diagram of the decoupled approach for VSGs. (a) the block diagram of active power-frequency, (b) the block diagram of reactive power-voltage

2.2. POWER ANGLE AND POWER FLOW EQUATIONS

Figure 3 shows the circuit diagram of a grid-connected VSG with the total reactance, resistance, and impedance of $X_{eq} = X_F + X_L$, $R_{eq} = R_L$, and $Z_{eq} = jX_{eq} + R_{eq}$, respectively. The active and reactive power injected by the inverter into the grid can be computed as:

$$P = \frac{1}{2}\left[\left(\frac{E^2}{Z_{eq}^2} - \frac{EV\cos\delta}{Z_{eq}^2}\right)R_{eq} + \frac{EV}{Z_{eq}^2}X_{eq}\sin\delta\right] \tag{4}$$

$$Q = \frac{1}{2}\left[\left(\frac{E^2}{Z_{eq}^2} - \frac{EV\cos\delta}{Z_{eq}^2}\right)X_{eq} - \frac{EV}{Z_{eq}^2}R_{eq}\sin\delta\right] \tag{5}$$

where the grid voltage, the inverter voltage, the injected active and reactive power, and the power angle are represented by V, E, P, Q, and δ, respectively. In inductive grids, such as high voltage grids, $X_{eq} \gg R_{eq}$, (4) and (5) can be simplified as:

$$P \approx \frac{EV}{2X_{eq}}\sin\delta \tag{6}$$

$$Q \approx \frac{E}{2X_{eq}}(\mathrm{E} - \mathrm{V}\cos\delta). \tag{7}$$

For the relatively small line inductance, the power angle is small; therefore, by simplifying expressions $\sin\delta$ and $\cos\delta$, (6) and (7) can be simplified as:

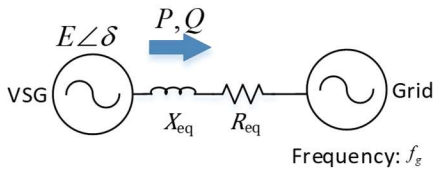

Figure 3. Equivalent circuit diagram of a grid connected VSG

$$P \approx \frac{EV}{2X_{eq}}\delta \tag{8}$$

$$Q \approx \frac{E}{2X_{eq}}(\mathrm{E}-\mathrm{V}). \tag{9}$$

Equations (8) and (9) authenticate the decoupled assumption in inductive grids. As it is shown, *P* can be controlled by the power angle and *Q* can be regulated by the magnitude of the inverter voltage, which confirms that the conventional VSGs are effective in inductive grids. conventional VSGs are based on the decoupled-control assumption. In other words, for conditions where the assumption is not valid, such as distributed systems and resistive/semi-resistive grids, conventional VSGs are unable to perform well. Besides, conventional VSGs are designed based on linear controller such as PI/I. In semi-resistive grids, the control loop is coupled. It means that the system is a multiple-input and multiple-output (MIMO). The linear controllers are not well suited for MIMO systems. Therefore, nonlinear control techniques such as feedback linearization or model predictive control can merge as potential replacements, but their behavior is highly dependent on the system model and the value of the parameters. However, a real power system with nonlinear elements, missing data parameters, and several uncertain conditions makes it infeasible to implement model-dependent techniques. Adaptive, model-free techniques can overcome the aforementioned drawbacks. An adaptive critic design technique based on the DHP is presented to regulate the power and frequency of a grid-connected VSG.

3. DUAL HEURISTIC DYNAMIC PROGRAMING

Adaptive critic design (ACD) techniques are neural-network-based optimization techniques. Besides, ACDs are well suited for noisy environment and system with uncertainties. The ACD was first introduced in [28] by combining the reinforcement learning technique and the dynamic programming technique. A typical ACD controller consists of two subnetworks: (i) the critic network and (ii) the action network. Some other types of ACDs also use a third model network. There are two methods to connect the action and critic network. The action network can be connected to the critic network directly, which is called an action-dependent ACD, or it can be connected through an identification model, which is called a model-dependent design. The ACD is based on Approximate Dynamic Programming (ADP). In other words, to penalized or reward (criticize) the agent (action network), the cost-to-go function is used. The critic neural network can be trained using the Bellman's equation which will be explained in this section. To train the action network, the derivative of the cost-to-function with respect to the state variables is required. The result of this concept is introduced as two main types of ACDs. The first type is the Value Learning (VL) technique in which the critic network objective is to approximate the value or cost-to-go function. Then, using the critic network and taking the derivative of the approximated value function the feedback signal can be generated to train the action network. The most common Value learning technique is the Heuristic Dynamic Programming technique. The second type of ACD is the Value Gradient Learning (VGL) in which the main objective of the critic function is to approximate the derivative of the value function with respect to the state variables

directly. The dual heuristic dynamic Programming (DHP) is the most common technique in VGLs. The main drawback of the VLs compared to the VGL is the slow training process due to search or optimal solution in the entire state. However, the VGL is much faster because it only requires scanning in the vicinity of the trajectory [29].

The main objective of the dynamic programming approach is to provide a control policy that minimizes a cost function over time. This cost function, which is a discounted cumulative utility function, $U(\cdot)$, is also known as cost-to-go function and can be computed as:

$$J(t) = \sum_{k=0}^{\infty} \gamma^k U(t+k). \tag{10}$$

A discount factor, $\gamma \in [0, 1]$, is defined to guarantee that the cost-to-go function is bounded. Besides, this factor determines the importance of the future costs. At any time $t=t_0$, by subtracting the cost function of the next time step $J(k+1)$ from the cost-to-go function $J(k)$ it can be written as:

$$J(k) = U(k) + \gamma J(k+1). \tag{11}$$

In this paper, the utility function is defined based on the active power error e_P, the reactive power error e_Q, and the rotational frequency error e_ω as:

$$U(k) = \sqrt{K_P e_P^2 + K_Q e_Q^2 + K_\omega e_\omega^2} \tag{12}$$

$$e_P = P_{set} - P \tag{13}$$

$$e_Q = Q_{set} - Q \tag{14}$$

$$e_\omega = \omega_g - \omega_i. \tag{15}$$

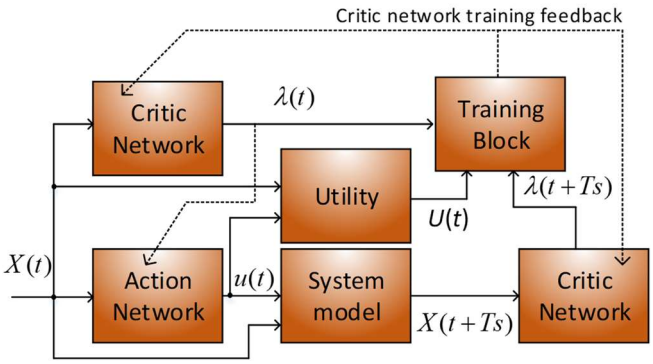

Figure 4. The block diagram of the proposed controller for VSG

The coefficients/weights K_P, K_Q, K_ω are defined to represent the importance of the active power, reactive power, and the frequency error, respectively. In dynamic programming techniques, computationally expensive techniques are used to compute the cost-to-go function. However, the ACDs use the neural network to estimate either the cost-to-go function or its derivative.

The block diagram of a DHP is illustrated in Figure 4. In this figure, the input vector to the action network and the output control vector is represented by $X(t)$ and $u(t)$, respectively. The critic network provides an estimation of the derivative of the cost-to-go function as the feedback signal for training the action network. The structure and the training procedure of the action network and the credit network are explained in this section. The feedback signal to train the critic and the action network is shown by the dotted lines.

3.1. CRITIC NEURAL NETWORK

In order to train the action network, a well-designed and well-trained critic network is required. As mentioned, the main objective of the critic network in DHPs is to

estimate the derivative of the cost-to-go function with respect to the control signal. By taking the derivative of both sides of (11), it can be written as:

$$\frac{\partial}{\partial X_i(t)} J(t) = \frac{\partial}{\partial X_i(t)} (U(t) + \gamma\, J(t+1)). \tag{16}$$

The required error signal to train the critic network can be defined as:

$$\|Er\| = \sum\nolimits_t e_c^T(t) e_c(t), \tag{17}$$

where $e_c(t)$ can be defined as:

$$e_c(t) = \frac{\partial}{\partial X(t)} J(t) - \frac{\partial}{\partial X(t)} \big(U(t) + \gamma\, J(t+1)\big). \tag{18}$$

Equation (10) can be rewritten by applying the chain rule as:

$$\frac{\partial J(t+1)}{\partial X_j(t)} = \sum_{i=1}^{n} \lambda_i(t+1) \frac{\partial X_i(t+1)}{\partial X_j(t)} + \sum_{k=1}^{m} \sum_{i=1}^{n} \lambda_i(t+1) \frac{\partial X_i(t+1)}{\partial u_k(t)} \frac{\partial u_k(t)}{\partial X_j(t)} \tag{19}$$

where the number of control signals and the number of states are represented by *m* and *n,* respectively. The expression $\lambda_i\ (t+1)$ can be defined as:

$$\lambda_i\ (t+1) = \frac{\partial J(t+1)}{\partial X_i\ (t+1)}$$

In this paper, the input signal to the action network is defined as $X = \big[P\ Q\ e_p\ e_q\ e_f\ \ \delta_i\big]$. Considering the important rule of the inverter power angle (δ_i) in defining the injected active/reactive power from the inverter into the power grid, the inverter power angle is being fed to the neural network as well. The input signal for the critic network can be defined as $Cr_{input} = [X\ E]$. By replacing (19) in (18), it can be rewritten as

$$e_{c_j}(t) = \frac{\partial J(t)}{\partial X_j(t)} - \frac{\partial}{\partial X(t)} \big(U(t) + \gamma\, J(t+1)\big). \tag{20}$$

The training signal for the critic network is expressed in (20). Either the exact model of the system or a neural network representing the system is required to compute the partial derivative of the next state with respect to the current state. In this paper, a neural network is used as a system identifier to estimate the state space model of the system. A fully connected, feedforward, neural network with one hidden layer consisting of seven neurons is used as the system identifier. To model the critic network, a multilayer, feedforward, fully connected neural network with two hidden layers and with four neurons at each layer is used.

3.2. ACTION NEURAL NETWORK

The main objective of the action network is to provide a set of controls to minimize the cost-to-go function for the immediate future. In other words, the goal is to minimize the discounted cumulative utility function for the infinite time horizon. To implement the action network, a fully connected, feedforward, multilayer NN is used. This neural network includes two hidden layers, and there are five neurons at each hidden layer. The backpropagation approach using the gradient decent technique is used to train the action network. The only difference between training the action network and a typical neural network is that the derivative of the cost-to-go function provided by the critic network is used as the error signal. As introduced in part A, the input of the action network is vector X, and the output of the action network is the peak value of the inverter voltage.

4. SIMULATION RESULTS

Figure 5 depicts the block diagram of the proposed DHP-based VSG. As explained in Section 3, the proposed DHP controller includes three neural networks: (i) the action network, (ii) the critic network, and (iii) the system identifier network. The system identifier neural network can be pretrained to perform as the model of the system. The action and the critic network are trained at each control cycle. The power meter block computes the active and reactive power transferred into the grid by reading the three-phase voltages and currents. A network input generator prepares the input vector X by receiving the active/reactive power and their references, and the frequency of the

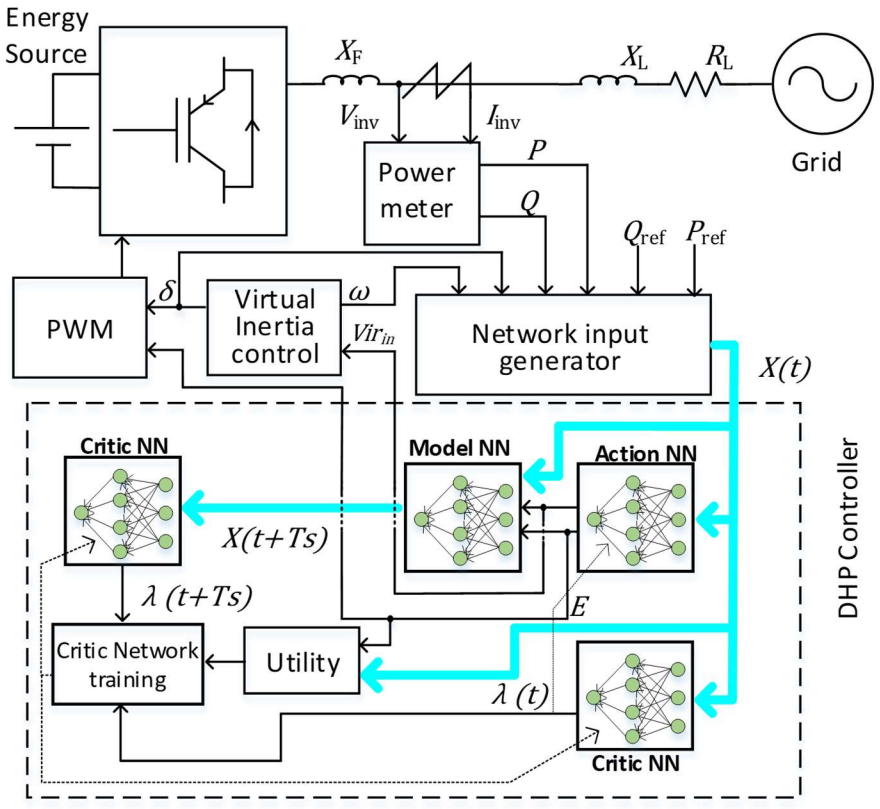

Figure 5. DHP-based synchronverter block diagram

inverter. The action network generates the optimal control signal, ($E\ (t)$), based on its input vector, and the input to the virtual inertia block ($Vir_{in}(t)$). Then, the critic network estimates the derivative of the cost-to-go function ($\lambda_i\ (t)$). The system identifier block is applied to predict the next states. The predicted next states are used to compute the next state control signal ($E\ (t + T_s)$). The predicted control and state signals are fed to the critic network to compute the next state output ($\lambda_i\ (t + T_s)$).

As discussed, conventional VSGs are unable to perform well in noninductive grids. To evaluate the effectiveness of the proposed DHP-based controller compared with a conventional VSG, the simulation results in both inductive and resistive grids are provided. The parameters of the grid and the VSG is provided in Table 1.

Table 1. System parameters used in simulation

Parameter	**Value**	**Unit**
DC voltage	250	V
AC line voltage	110	V
AC frequency	60	Hz
Moment of inertia	0.1	Kg.m2
Frequency droop	%4	--
Inverter power rating	5	kW
Inductive line		
Filter inductance	1	µH
Line inductance	100	µH
Line resistance	10	mΩ
Resistive line		
Filter inductance	1	µH
Line inductance	1	µH
Line resistance	500	mΩ
DHP parameters		
γ	1	
Sampling time	1	ms
$[k_P\ \ k_Q\ \ k_f]$	[1 1 0]	--

4.1. INDUCTIVE GRID

In Section 2, it is discussed that the conventional VSG is designed based on inductive grid assumption. In other words, a well-designed PI-based VSG can perform well in inductive grids. In this section, active and reactive power reference changes are applied to both the conventional and the DHP-based VSGs. As the simulation results show, and as it was expected from the mathematical point of view, the conventional performance is acceptable in tracking the power references. The DHP-based VSG performs an optimal response in tracking the power references. The performance of the DHP-based VSG is slightly better than the conventional VSG for two reasons: (i) the conventional VSG are designed based on inductive connections and the simulation is for a semi-inductive grid, and (ii) the PI parameters in the VSG is designed for the nominal operating point and the alteration in the operating point reduces the effectiveness of the conventional VSG. On the other hand, the reinforcement learning characteristic of the DHP enables the controller to adjust itself with the line impedance and different operating point conditions. Figure 6 illustrates the performance of the conventional and DHP-based controller.

4.2. RESISTIVE GRID

As analyzed in Section 2, the conventional VSG design is not well suited for noninductive grids. In noninductive grids, the decoupled control assumption is no longer valid and extremely affects the performance of the VSG. In this part, the performance of the DHP-based VSG is compared with the conventional VSG to evaluate the effectiveness of the proposed approach. The simulation results illustrate that the

conventional VSG is unable to perform well in tracking the active and reactive power references, because it only utilizes the frequency to control the power, and the magnitude of the voltage to control the reactive power, which is not the case in resistive/noninductive grids. The main goal of the VSG is to improve the dynamics of the inverter, however as shown in Figure 6, the performance is far from optimal. One method is to switch the controller platform to the conventional direct power direct current controller, which would have the main two drawbacks of inertia-less and PLL requirement. In the second approach, the proposed controller based on the value gradient is used to improve the dynamics while maintaining the advantages of inertia-based and PLL-less. The performance of the conventional VSG is nonoptimal and includes oscillations in the output power. On the other hand, the DHP-based VSG tracks the power references smoothly, because it uses both active and reactive power error to regulate the

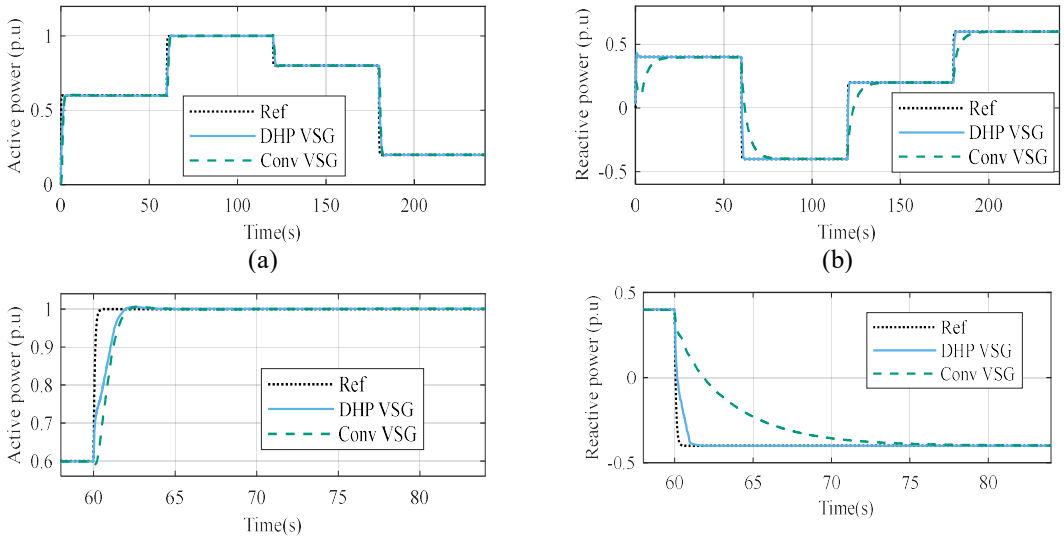

Figure 6. The performance of the DHP-based VSG and the conventional PI-based VSG in an inductive grid(a) active power (b) reactive power (c) active power (zoomed in) (d) reactive power (zoomed in)

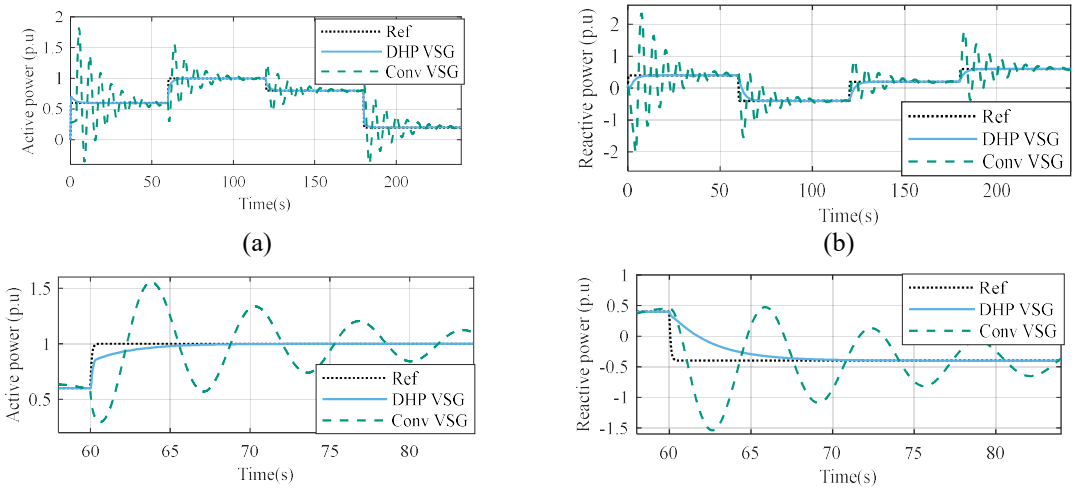

Figure 7. The performance of the DHP-based VSG and the conventional PI-based VSG in a resistive grid (a) active power (b) reactive power (c) active power (zoomed in) (d) reactive power (zoomed in)

inverter voltage. The active and reactive power signals for the conventional and DHP-based VSGs are depicted in Figure 7.

5. EXPERIMENTAL RESULTS

To evaluate the effectiveness of the proposed approach, a laboratory prototype is prepared. The prototype is a 1VA grid-connected VSG. The inverter is connected to a three-phase grid with the line-line voltage of 190V/60Hz. The control block diagram includes two parts: (i) the embedded controller, which is implemented by a Texas Instruments (TI) digital signal processor (DSP), TMS320F28377, and (ii) MATLAB R2018. The embedded controller includes the direct current control and conventional VSG. The DHP-based control scheme is utilized by a computer using MATLAB. Figure 8 illustrates the prototype. As discussed earlier, to provide enough power during

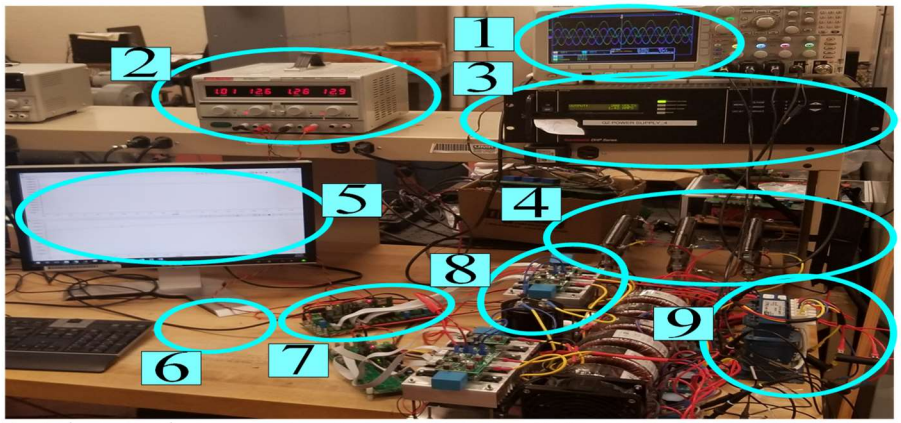

1. Three-phase output
2. DC supply for Control
3. DC storage for DC side
4. Three-phase load
5. Online monitoring
6. Serial communication
7. TI microprocessor
8. Driver & switching board
9. Emulated resistive line

Figure 8. Three-phase grid-connected inverter test bed

transients, the dc side is connected to a dc power supply. A three-phase transformer is implemented in the output side of the inverter to provide the electrical isolation and to boost up the voltage. A three-phase relay connects the inverter into the grid. The DSP communicates with the computer via a USB2SERIAL adaptor. The current and voltage signals are read by the embedded analog to digital converter (ADC) in the DSP. The DSP is responsible to generate the PWM signals based on the magnitude and the phase of the voltage provided by each one of controllers. The neural networks presenting the action network, critic network and system identifier are trained every 1 millisecond. The action network generates the control signal at every control cycle.

5.1. TRAINING THE NETWORKS

As discussed earlier, the proposed technique includes three neural networks. The first neural network is the system identifier. The model neural network estimates the behavior of the model of the system to predict the next state of the system. This network

Algorithm I. HDP-based controller
• Prepare state variables: Read the current and the output voltage of the inverter and compute the injected active/reactive power • Generate the neural network input vector • Train the pretrained model neural network • Feed the states to the action network and generate the output • Feed the outputs of the action network to the PWM block and the swing equation block • Compute the utility function • Feed the state vector to the system neural network and estimate the next state vector • Compute the current and the next state Lambda and generate the error signal for the critic network • Train and update the critic network • Using the critic network train and update the action network

does not depend on the controller, and it is pretrained using a conventional VSG. After the model network is trained, the critic network is pretrained to smoothen the training of the action network. Lastly, the action network can be trained online, and all the parameters for the critic and the model network can be trained forward in time. It is shown in Algorithm I.

To train the model network, the state of the inverter and the control signal of the inverter form an input vector for the neural network. The states' values for the next time step are the output of the neural network. This network is pretrained offline by the 10000 samples of collected data.

To train the critic network, as explained in Section 3, the error signal is required. To compute the error signal, the derivative signal for the current state and the next state is required. The next state estimation can be generated by the model network and be fed to the critic network to generate the output for the next step. The output of the critic network

plays a significant rule in training the action network. To enhance the performance of the proposed controller, the critic network is also pretrained in advance. The mathematical equations to update the critic network is expressed by (16)-(20). Another approach in training the critic network is to train the critic network simultaneously with the action network. The training procedure for the action network is much faster in the first approach.

To train the action network, the feedback signal from the critic network is required. Similar to the critic network and the `millisecond. The regular backpropagation technique using the gradient decent is used to train the action network.

5.2. RESISTIVE GRID CONNECTION

As discussed earlier, the performance of the conventional VSG in inductive grids are acceptable, and the simulation results confirm that. On the other hand, the conventional VSG performance in noninductive grids is nonoptimal, which is confirmed

Table 2. Experimental test bed parameters

Parameter	Value	Unit
VSG		
DC voltage	400	V
AC line voltage	110	V
AC frequency	60	Hz
Moment of inertia	0.5	Kg. m2
Frequency droop	%4	--
Inverter power rating	1	kW
Line Parameters		
Filter reactance	900	mΩ
Line reactance	150	mΩ
Line resistance	1800	mΩ

by the simulation results. Therefore, in this part, the behavior of the VSG in a resistive grid is only evaluated. The parameters of the prototype are illustrated in Table 2.

In the first part of the experiment, the reactive power reference is fixed in 0.1 (p.u), and the active power reference changes in {0.1, 0.05, 0.2, 0.4, 0.1, 0.2, 0.1} (p.u). Figure 10 illustrates the inverter's current and voltage when it faces a change in the active power reference. As shown, the inverter voltage and the inverter phase change to regulate the power. The output active and reactive power is shown in Figure 9. In this figure, the active power and reactive power are shown by green (top) and blue (bottom) waveform, respectively. The active and reactive power output are generated as analog signals in a range of zero to five volts. The power compute unit maps the active power in range of [-1000,1000] (W) to [0,5] (V), and the reactive power in range of [-700,700] (VAR) to [0,5] (V). In this figure, the conventional VSG performance facing changes in the active power is shown in (a), and the magnified view is shown in (b). To compare the results with the proposed DHP-based VSG controller, figure (c) illustrates the performance of

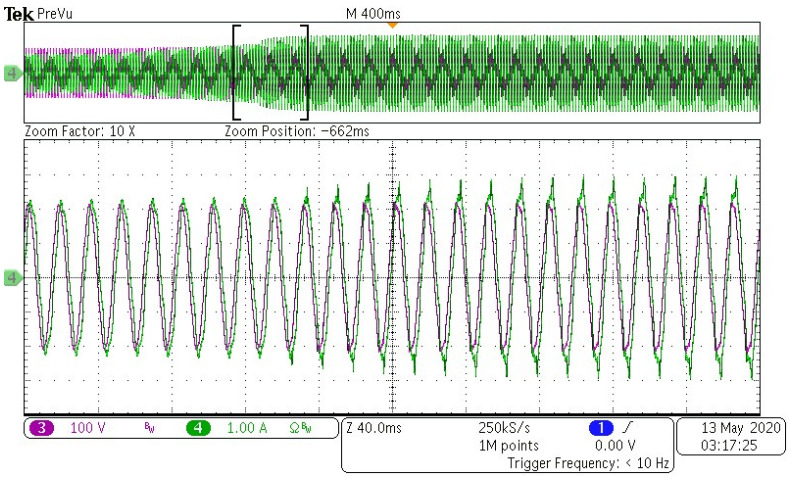

Figure 9. The phase output voltage and the line current of synchronverter after the low-pass filter

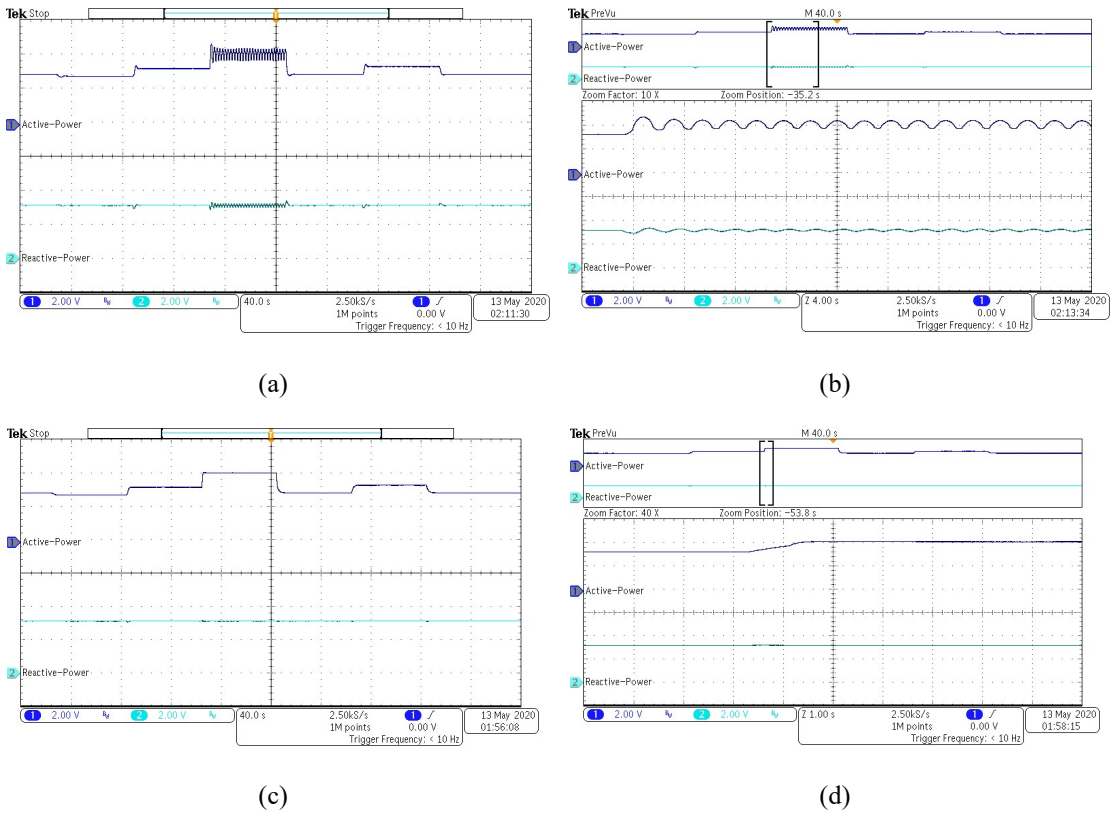

Figure 10. Injected active and reactive power from a three-phase grid connected synchronverter facing active power reference changes (a) traditional VSG, (b) magnified response for traditional VSG, (c) HDP-based VSG (d) magnified waveform of HDP-based VS

the DHP-based VSG facing the same changes in active power references. The magnified version is illustrated in figure (d).

As expected, based on the analytical computation in Section 2, and the simulation results in Section 4, the conventional VSG is not well-suited for the resistive grids and generates oscillation in active and reactive power. In contrast, the DHP-based VSG tracks the power references smoothly.

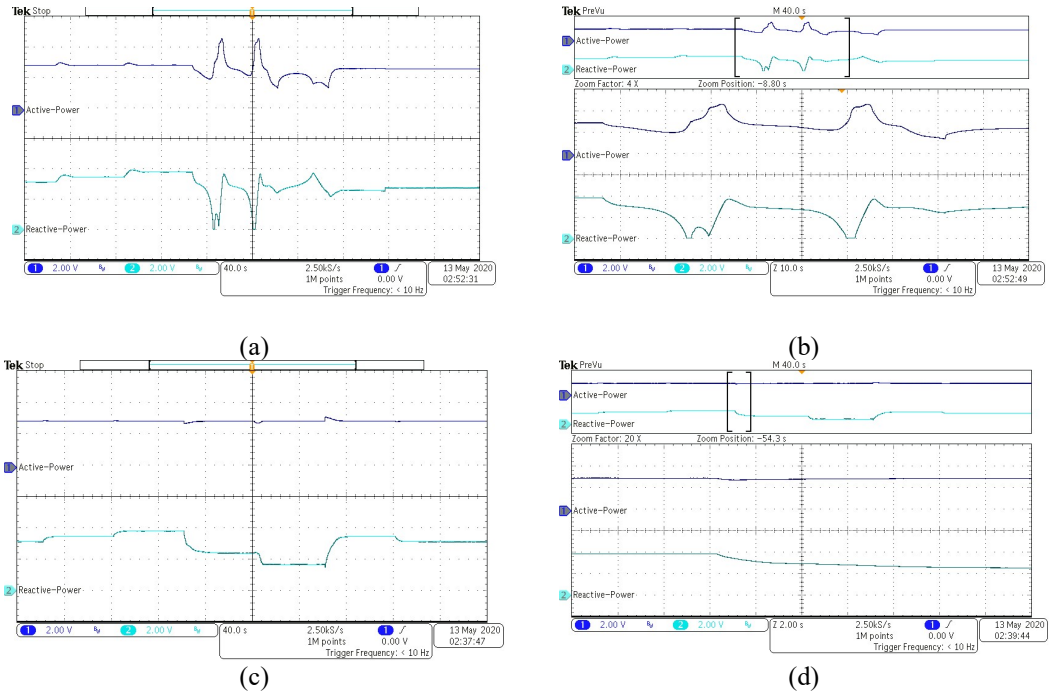

Figure 11. Injected active and reactive power from a three-phase grid connected synchronverter facing reactive power reference changes (a) traditional VSG, (b) magnified response for traditional VSG, (c) HDP-based VSG (d) magnified output waveform of HDP-based VSG

In the second part of the experiment, the active power reference is fixed in 0.1 (p.u) and the reactive reference changes in {0.1, 0.2, 0.3, -0.05, -0.2, 0.2, 0.1} (p.u). The output active and reactive power of the inverter is shown in Figure 11. As shown in this experiment, the conventional VSG is unstable, and the system goes to instability. It is important to mention this point that since the conventional VSGs are based on linear controllers, they depend on the linearized model around the operating point. In other words, a stable controller in some operating point can go to instability in another operating point. The nonlinearity of the filter inductor and transformer in the laboratory prototype escalates this concern. The experimental results highlight the weakness of the conventional VSGs. The DHP-based VSG tracks the references with much less

oscillations and with lower overshoots. The adaptation characteristic of DHP-based VSG guarantees optimal performance in regulating the voltage and the frequency while tracking the active and the reactive references.

6. CONCLUSION

Grid-connected inverters are widely used to connect renewable energy resources into the power grid. The fast-responding inertia-less inherence of these power electronics converters significantly affects the power system stability. The concept of the virtual synchronous generator is a suitable replacement for the conventional controller. This approach improves the power system's stability, but it is designed for inductive grids, and it is not optimal for noninductive grids such as low voltage grids. To overcome this drawback, a reinforcement learning-based controller is introduced in this paper to regulate the power and the frequency of a grid-connected VSG. A dual heuristic dynamic programming approach is presented in this paper to optimally control the transmitted power into the grid by adjusting the voltage and frequency of the inverter. The proposed approach is simulated in MATLAB in both inductive and resistive grids to confirm its effectiveness compared to a conventional VSG. A laboratory prototype is provided to confirm the feasibility of the proposed approach. As the simulation and experimental results confirm, the proposed approach demonstrates better performance while facing different power angles in various operating points.

REFERENCES

[1] F. Blaabjerg, R. Teodorescu, M. Liserre, and A. V. Timbus, "Overview of control and grid synchronization for distributed power generation systems," *IEEE Transactions on Industrial Electronics*, vol. 53, no. 5. pp. 1398–1409, Oct. 2006, doi: 10.1109/TIE.2006.881997.

[2] Q. C. Zhong, "Power-Electronics-Enabled Autonomous Power Systems: Architecture and Technical Routes," *IEEE Trans. Ind. Electron.*, vol. 64, no. 7, pp. 5907–5918, Jul. 2017, doi: 10.1109/TIE.2017.2677339.

[3] H. Bevrani, T. Ise, and Y. Miura, "Virtual synchronous generators: A survey and new perspectives," *Int. J. Electr. Power Energy Syst.*, vol. 54, pp. 244–254, Jan. 2014, doi: 10.1016/j.ijepes.2013.07.009.

[4] B. Silva, C. L. Moreira, L. Seca, Y. Phulpin, and J. A. P. Lopes, "Provision of inertial and primary frequency control services using offshore multiterminal HVDC networks," *IEEE Trans. Sustain. Energy*, vol. 3, no. 4, pp. 800–808, 2012, doi: 10.1109/TSTE.2012.2199774.

[5] A. Asrari, M. Mustafa, M. Ansari, and J. Khazaei, "Impedance Analysis of Virtual Synchronous Generator-Based Vector Controlled Converters for Weak AC Grid Integration," *IEEE Trans. Sustain. Energy*, vol. 10, no. 3, pp. 1481–1490, Jul. 2019, doi: 10.1109/TSTE.2019.2892670.

[6] Z. Miao, L. Fan, D. Osborn, and S. Yuvarajan, "Wind farms with HVdc delivery in inertial response and primary frequency control," *IEEE Trans. Energy Convers.*, vol. 25, no. 4, pp. 1171–1178, Dec. 2010, doi: 10.1109/TEC.2010.2060202.

[7] S. Golestan, M. Monfared, F. D. Freijedo, and J. M. Guerrero, "Advantages and challenges of a type-3 PLL," *IEEE Trans. Power Electron.*, vol. 28, no. 11, pp. 4985–4997, 2013, doi: 10.1109/TPEL.2013.2240317.

[8] Q. C. Zhong and G. Weiss, "Synchronverters: Inverters that mimic synchronous generators," *IEEE Trans. Ind. Electron.*, vol. 58, no. 4, pp. 1259–1267, Apr. 2011, doi: 10.1109/TIE.2010.2048839.

[9] H. P. Beck and R. Hesse, "Virtual synchronous machine," 2007, doi: 10.1109/EPQU.2007.4424220.

[10] J. Driesen and K. Visscher, "Virtual synchronous generators," 2008, doi: 10.1109/PES.2008.4596800.

[11] M. Torres and L. A. C. Lopes, "Virtual synchronous generator control in autonomous wind-diesel power systems," 2009, doi: 10.1109/EPEC.2009.5420953.

[12] F. Nejabatkhah and Y. W. Li, “Overview of Power Management Strategies of Hybrid AC/DC Microgrid,” *IEEE Transactions on Power Electronics*, vol. 30, no. 12. Institute of Electrical and Electronics Engineers Inc., pp. 7072–7089, Dec. 01, 2015, doi: 10.1109/TPEL.2014.2384999.

[13] Q. C. Zhong and G. Weiss, “Static synchronous generators for distributed generation and renewable energy,” 2009, doi: 10.1109/PSCE.2009.4840013.

[14] T. Shintai, Y. Miura, and T. Ise, “Oscillation damping of a distributed generator using a virtual synchronous generator,” *IEEE Trans. Power Deliv.*, vol. 29, no. 2, pp. 668–676, 2014, doi: 10.1109/TPWRD.2013.2281359.

[15] X. Meng, J. Liu, and Z. Liu, “A Generalized Droop Control for Grid-Supporting Inverter Based on Comparison between Traditional Droop Control and Virtual Synchronous Generator Control,” *IEEE Trans. Power Electron.*, vol. 34, no. 6, pp. 5416–5438, Jun. 2019, doi: 10.1109/TPEL.2018.2868722.

[16] J. Chen and T. O’Donnell, “Parameter constraints for virtual synchronous generator considering stability,” *IEEE Trans. Power Syst.*, vol. 34, no. 3, pp. 2479–2481, May 2019, doi: 10.1109/TPWRS.2019.2896853.

[17] W. Du, Q. Fu, and H. F. Wang, “Power System Small-Signal Angular Stability Affected by Virtual Synchronous Generators,” *IEEE Trans. Power Syst.*, vol. 34, no. 4, pp. 3209–3219, Jul. 2019, doi: 10.1109/TPWRS.2019.2896149.

[18] A. Karimi *et al.*, “Inertia Response Improvement in AC Microgrids: A Fuzzy-Based Virtual Synchronous Generator Control,” *IEEE Trans. Power Electron.*, vol. 35, no. 4, pp. 4321–4331, Apr. 2020, doi: 10.1109/TPEL.2019.2937397.

[19] K. Shi, H. Ye, W. Song, and G. Zhou, “Virtual Inertia Control Strategy in Microgrid Based on Virtual Synchronous Generator Technology,” *IEEE Access*, vol. 6, pp. 27949–27957, May 2018, doi: 10.1109/ACCESS.2018.2839737.

[20] A. Fathi, Q. Shafiee, and H. Bevrani, “Robust frequency control of microgrids using an extended virtual synchronous generator,” *IEEE Trans. Power Syst.*, vol. 33, no. 6, pp. 6289–6297, Nov. 2018, doi: 10.1109/TPWRS.2018.2850880.

[21] M. Choopani, S. H. Hosseinian, and B. Vahidi, “New Transient Stability and LVRT Improvement of Multi-VSG Grids Using the Frequency of the Center of Inertia,” *IEEE Trans. Power Syst.*, vol. 35, no. 1, pp. 527–538, Jan. 2020, doi: 10.1109/TPWRS.2019.2928319.

[22] J. Li, B. Wen, and H. Wang, “Adaptive virtual inertia control strategy of VSG for micro-grid based on improved bang-bang control strategy,” *IEEE Access*, vol. 7, pp. 39509–39514, 2019, doi: 10.1109/ACCESS.2019.2904943.

[23] S. Saadatmand, P. Shamsi, and M. Ferdowsi, “Power and Frequency Regulation of Synchronverters Using a Model Free Neural Network–Based Predictive Controller,” *IEEE Trans. Ind. Electron.*, pp. 1–1, Apr. 2020, doi: 10.1109/tie.2020.2984419.

[24] R. Shi, X. Zhang, C. Hu, H. Xu, J. Gu, and W. Cao, “Self-tuning virtual synchronous generator control for improving frequency stability in autonomous photovoltaic-diesel microgrids,” *J. Mod. Power Syst. Clean Energy*, vol. 6, no. 3, pp. 482–494, May 2018, doi: 10.1007/s40565-017-0347-3.

[25] F. Wang, L. Zhang, X. Feng, and H. Guo, “An Adaptive Control Strategy for Virtual Synchronous Generator,” *IEEE Trans. Ind. Appl.*, vol. 54, no. 5, pp. 5124–5133, Sep. 2018, doi: 10.1109/TIA.2018.2859384.

[26] S. Saadatmand, P. Shamsi, and M. Ferdowsi, “Adaptive critic design-based reinforcement learning approach in controlling virtual inertia-based grid-connected inverters,” *Int. J. Electr. Power Energy Syst.*, vol. 127, p. 106657, May 2021, doi: 10.1016/j.ijepes.2020.106657.

[27] S. Saadatmand, M. S. S. Nia, P. Shamsi, and M. Ferdowsi, “Dual heuristic dynamic programing control of grid-connected synchronverters,” Feb. 2020, pp. 1–6, doi: 10.1109/naps46351.2019.9000382.

[28] WERBOS and P., “Approximate dynamic programming for realtime control and neural modelling,” *Handb. Intell. Control neural, fuzzy Adapt. approaches*, pp. 493–525, 1992.

[29] D. V. Prokhorov and D. C. Wunsch, “Adaptive critic designs,” *IEEE Trans. Neural Networks*, vol. 8, no. 5, pp. 997–1007, 1997, doi: 10.1109/72.623201.

SECTION

2. CONCLUSIONS AND RECOMMENDATIONS

The increase in penetration of renewable energy sources as distributed generations (DGs) has increased the integration of fast-responding inertia-less power electronics converter. The conventional grid-connected inverters are controlled through the direct current control scheme, which affects the stability of the power system, in particular in weak grids. The concept of the virtual synchronous generator has been introduced to address these concerns by mimicking the mechanical behavior of synchronous generators. However, the conventional VSG has two main drawbacks: (i) this method is unable to perform optimally in resistive grids, and (ii) the conventional VSG is designed based on linear controllers, which is not suitable for varying operating point. Three approaches are proposed in this research to address the aforementioned drawbacks. In the first approach the NNPC is proposed to regulate the voltage and frequency of a grid-connected VSG. This method addresses the conventional VSG drawback; however, it only optimizes the cost function for a specific time horizon. In the second approach the HDP-based VSG is proposed to control the grid-connected inverter, which optimizes the cost function for an infinite time horizon. Nevertheless, the training procedure is time consuming because the critic neural network requires to search the entire state space. Therefore, in the third approach, a DHP-based VSG is proposed to perform as an approximate dynamic programming with a faster training rate. The simulation and

experimental results are provided to evaluate the effectiveness of the proposed approaches, and the results are compared with the conventional VSG performance when facing active and reactive power reference changes.

REFERENCES

[1] F. Blaabjerg, R. Teodorescu, M. Liserre, and A. V. Timbus, "Overview of control and grid synchronization for distributed power generation systems," *IEEE Transactions on Industrial Electronics*, vol. 53, no. 5. pp. 1398–1409, Oct. 2006, doi: 10.1109/TIE.2006.881997.

[2] Q. C. Zhong, "Power-Electronics-Enabled Autonomous Power Systems: Architecture and Technical Routes," *IEEE Trans. Ind. Electron.*, vol. 64, no. 7, pp. 5907–5918, Jul. 2017, doi: 10.1109/TIE.2017.2677339.

[3] H. Bevrani, T. Ise, and Y. Miura, "Virtual synchronous generators: A survey and new perspectives," *Int. J. Electr. Power Energy Syst.*, vol. 54, pp. 244–254, Jan. 2014, doi: 10.1016/j.ijepes.2013.07.009.

[4] B. Silva, C. L. Moreira, L. Seca, Y. Phulpin, and J. A. P. Lopes, "Provision of inertial and primary frequency control services using offshore multiterminal HVDC networks," *IEEE Trans. Sustain. Energy*, vol. 3, no. 4, pp. 800–808, 2012, doi: 10.1109/TSTE.2012.2199774.

[5] A. Asrari, M. Mustafa, M. Ansari, and J. Khazaei, "Impedance Analysis of Virtual Synchronous Generator-Based Vector Controlled Converters for Weak AC Grid Integration," *IEEE Trans. Sustain. Energy*, vol. 10, no. 3, pp. 1481–1490, Jul. 2019, doi: 10.1109/TSTE.2019.2892670.

[6] Z. Miao, L. Fan, D. Osborn, and S. Yuvarajan, "Wind farms with HVdc delivery in inertial response and primary frequency control," *IEEE Trans. Energy Convers.*, vol. 25, no. 4, pp. 1171–1178, Dec. 2010, doi: 10.1109/TEC.2010.2060202.

[7] S. Golestan, M. Monfared, F. D. Freijedo, and J. M. Guerrero, "Advantages and challenges of a type-3 PLL," *IEEE Trans. Power Electron.*, vol. 28, no. 11, pp. 4985–4997, 2013, doi: 10.1109/TPEL.2013.2240317.

[8] Q. C. Zhong and G. Weiss, "Synchronverters: Inverters that mimic synchronous generators," *IEEE Trans. Ind. Electron.*, vol. 58, no. 4, pp. 1259–1267, Apr. 2011, doi: 10.1109/TIE.2010.2048839.

[9] H. P. Beck and R. Hesse, "Virtual synchronous machine," 2007, doi: 10.1109/EPQU.2007.4424220.

[10] M. Torres and L. A. C. Lopes, "Virtual synchronous generator control in autonomous wind-diesel power systems," 2009, doi: 10.1109/EPEC.2009.5420953.

[11] S. Saadatmand, P. Shamsi, and M. Ferdowsi, “Power and Frequency Regulation of Synchronverters Using a Model Free Neural Network–Based Predictive Controller,” *IEEE Trans. Ind. Electron.*, pp. 1–1, Apr. 2020, doi: 10.1109/tie.2020.2984419.

[12] S. Saadatmand, M. S. S. Nia, P. Shamsi and M. Ferdowsi. “Neural Network Predictive Controller for Grid-Connected Virtual Synchronous Generator,” in *North American Power Symposium (NAPS)*, 2019. IEEE, 2019, pp. 1–6

[13] S. Saadatmand, P. Shamsi, and M. Ferdowsi, “Adaptive critic design-based reinforcement learning approach in controlling virtual inertia-based grid-connected inverters,” *Int. J. Electr. Power Energy Syst.*, vol. 127, p. 106657, May 2021, doi: 10.1016/j.ijepes.2020.106657.

[14] S. Saadatmand, M. S. S. Nia, P. Shamsi and M. Ferdowsi. “Heuristic Dynamic Programming for Adaptive Virtual Synchronous Generators,” in *North American Power Symposium (NAPS)*, 2019. IEEE, 2019, pp. 1– 6

[15] S. Saadatmand, M. S. S. Nia, P. Shamsi, and M. Ferdowsi, “Dual heuristic dynamic programing control of grid-connected synchronverters,” Feb. 2020, pp. 1–6, doi: 10.1109/naps46351.2019.9000382.

[16] S. Saadatmand, H. Alharkan, P. Shamsi, M. Ferdowsi, Value Gradient Learning Approach in Power and Frequency Regulation of Grid-Connected Synchronverters, *IEEE Power and Energy Conference at Illinois (PECI)* (2020) 1-6

[17] S. Saadatmand, P. Shamsi, and M. Ferdowsi, “The Active and Reactive Power Regulation of Grid-Connected Virtual Inertia-Based Inverters Based on the Value Gradient Learning,” *IEEE Journal of Emerging and Selected Topics in Industrial Electronics*.

VITA

Sepehr Saadatmand received the B.Sc. degree from the Amirkabir University of Technology, Tehran, Iran, the first M.Sc. degree from the University of Tehran, Tehran, Iran, and the second M.Sc. degree from the Southern Illinois University, Carbondale, USA, all in electrical engineering. He worked as Graduate Research Assistant with the subject of " Advanced Control Techniques for Modern Inertia Based Inverters". His research interests included the application of control and machine learning in power electronics and distributed energy resources. In July 2021, he received his Ph.D. degree in Electrical Engineering from Missouri University of Science and Technology, Rolla, MO, USA.